Virginia Commonwealth University
VCU Scholars Compass

Theses and Dissertations

Graduate School

1994

Characterization of fibroblasts with a unique defect in processing antigens with disulfide bonds

Brian J. Merkel

Follow this and additional works at: https://scholarscompass.vcu.edu/etd

Part of the Microbiology Commons

© The Author

Downloaded from
https://scholarscompass.vcu.edu/etd/5076

This Dissertation is brought to you for free and open access by the Graduate School at VCU Scholars Compass. It has been accepted for inclusion in Theses and Dissertations by an authorized administrator of VCU Scholars Compass. For more information, please contact libcompass@vcu.edu.

Virginia Commonwealth University
School of Medicine

This is to certify that the dissertation prepared by Brian J. Merkel entitled "Characterization of Fibroblasts with a Unique Defect in Processing Antigens with Disulfide Bonds" has been approved by his committee as satisfactory completion of the dissertation requirement for the degree of Doctor of Philosophy.

[redacted]
Kathleen L. McCoy, Ph.D., Director of Dissertation

[redacted]
Francine Marciano-Cabral, Ph.D., School of Medicine

[redacted]
Joseph Liberti, Ph.D., School of Medicine

[redacted]
Anthony Carter, Ph.D., School of Medicine

[redacted]
Suzanne Barbour, Ph.D., School of Medicine

[redacted]
Francis Macrina, Ph.D., Department Chairman

[redacted]
Hermes A. Kontos, M.D., Ph.D., Dean, School of Medicine

[redacted]
William L. Dewey, Ph.D., Dean, School of Graduate Studies

December 9, 1994
Date

Characterization of fibroblasts with a unique defect in processing antigens with disulfide bonds

A dissertation in submitted in partial fulfillment of the
requirements for the degree of Doctor of Philosophy
at Virginia Commonwealth University

By

Brian J. Merkel
B.A. University of Richmond, May 1989

Director: Kathleen L. McCoy, Ph.D.
Associate Professor
Department of Microbiology and Immunology

Virginia Commonwealth University
Richmond, Virginia
December, 1994

ACKNOWLEDGMENTS

I would like to acknowledge the invaluable contribution of my advisor Dr. Kathy McCoy without whom this work would not have been possible. I would also like to thank the members of my committee: Drs. Francine Marciano-Cabral, Joseph Liberti, Anthony Carter, and Suzanne Barbour for their guidance during the course of my training. Finally, my family and friends have always supported me and have my sincerest gratitude.

TABLE OF CONTENTS

Page

LIST OF TABLES v

LIST OF FIGURES vi

ABBREVIATIONS vii

ABSTRACT iX

INTRODUCTION 1

Cell-mediated immunity 2
Molecules of the major histocompatibility complex 2
T cell recognition of peptide and MHC 3
MHC class I presentation 10
MHC class II presentation 12
Lysosomal reductive cleavage mechanism 18
Rationale and objectives 19

MATERIALS AND METHODS 23

Cell lines 23
Ag and mAb 23
T cell stimulation assay 24
Somatic cell hybrid generation 25
Karyotypic analysis 25
Cloning of hybrid cells 25
Immunofluorescence staining and flow cytometry 25
Aspartic acid protease assay 26
Endoglycosidase H removal of carbohydrate residues 27
Separation of glycosylated and unglycosylated OVA 27
Enzyme-linked immunoabsorbant assay of glycosylated OVA 28
Disulfide bond reduction of Ag 28
Circular dichroism 29
Cellular disulfide reductive function 29
Intracellular levels of cysteine and GSH 30
Cysteine transporter activity 31
Inhibition of glutathione synthesis 32
N-acetyl cysteine treatment of WAB4 cells 32

RESULTS 34

Limited defect of WAB4 cells in Ag processing 34
WAB4 cells present peptides 37
The defect of WAB4 cells is recessive 37
Karyotypic analysis of the WALC hybrid population 42
A limited number of genes mediates the defect observed in WAB4 cells 42
MHC class II expression by hybrid clones 46
Surface expression of MHC class I

molecules by hybrid clones 50
Invariant chain expression 53
Normal levels of aspartic acid proteolytic activity 53
The effect of carbohydrate residues on the processing of OVA by WAB4 cells 56
Reduction of OVA and HEL restores normal processing by WAB4 61
Decreased cleavage of disulfide bonds 69
Intracellular levels of cysteine and glutathione 72
Cysteine transporter activity 74
Inhibition of glutathione synthesis in WALC hybrid cells 74
N-acetyl cysteine treatment of WAB4 cells 77

DISCUSSION 81

LITERATURE CITED 90

VITA 99

LIST OF TABLES

Table Page

1 Karyotypic analysis of the WALC hybrid population and parental WAB4 cells and L cells 43

2 Representation of hamster chromosomes among WALC hybrids 44

3 Antigen processing phenotypes among WALC clones 45

4 Mode fluorescence intensity of MHC class II expression among WALC clones 47

5 Correlation of presence of disulfide bonds in the Ag processing defect of WAB4 cells 62

6 Intracellular levels of GSH and cysteine 73

7 BSO treatment of WALC hybrid cells 78

8 N-acetyl treatment of WAB4 cells 80

LIST OF FIGURES

Figure Page

1 Peptide-binding groove of the human HLA-A2 class I molecule 5

2 Peptide-binding groove of the human HLA-DR1 class II molecule 7

3 Schematic illustration of APC-mediated T_h cell activation 9

4 Model for MHC class II presentation of exogenously-derived peptides 14

5 Lysosomal reductive cleavage mechanism 21

6 T cells specific for Ag processing disulfide bonds are not activated by WAB4 cells 36

7 Normal peptide presentation by WAB4 cells 39

8 Rescue of Ag processing by genetic complementation 41

9 Dot plot analysis of MHC class II (Ia) expression and processing efficiency among WALC hybrid clones 49

10 MHC class I H-$2K^kD^k$ expression among WALC clones 52

11 Low expression of the Ii chain cytoplasmic domain epitope In-1 by APC 55

12 WAB4 cells possess normal levels of aspartyl proteolytic activity 58

13 Endoglycosidase-H treatment of OVA 60

14 Extensive loss of secondary structure of OVA after reduction . 64

15 Circular dichroism analysis of HEL 66

16 Restoration of processing by reduction of OVA and HEL 68

17 Diminished reduction of disulfide bonds 71

18 Cysteine-specific transporter activity in WAB4 and 125 hybrid cells 76

ABBREVIATIONS

Antigen (Ag)

Antigen-presenting cell (APC)

2,2′-azino-bis(3-ethylbenzthiazoline (ABTS)

B2 microglobulin (β_2M)

Buthionine Sulfoximine (BSO)

Carboxymethylated hen egg lysozyme (CM-HEL)

Carboxymethylated ovalbumin (CM-OVA)

Chinese hamster ovary cell (CHO)

Class II-associated invariant chain peptide (CLIP)

Compartment for peptide loading (CPL)

Concanavalin A (Con A)

Cysteine (Cys)

Denatured ovalbumin (D-OVA)

5,5′-dithiobis-(nitrobenzoic) acid (DTNB)

Endoglycosidase-H (Endo H)

Endoplasmic reticulum (ER)

Enzyme linked immunoabsorbant assay (ELISA)

Fluorescein isothiocyanate (FITC)

Geneticin (G418)

Hank's balanced salt solution (HBSS)

hen egg lysozyme (HEL)

Hour (h)

Iodinated tyramine disulfide linked to polymer of D-Lysine (^{125}I-tyn-SS-PDL)

Interleukin (IL)

Invariant chain (Ii)

Kilodalton (Kd)

Low molecular weight polypeptide complex (LMP)

Major histocompatibility complex (MHC)

Minutes (min)

Monoclonal antibody (mAb)

N-acetyl cysteine (NAC)

Nicotinamide adenine dinucleotide phosphate (NADPH)

N-ethylmaleimide (NEM)

Ovalbumin (OVA)

Oxidized glutathione (GSSG)

Polyethylene glycol (PEG)

Phosphate buffered saline (PBS)

Reduced glutathione (GSH)

Sodium dodecyl sulfate polyacrylamide gel electrophoresis (SDS-PAGE)

Suppressor T cell (T_s)

T cell receptor (TCR)

T helper cell (T_h)

2-nitro-5-thiobenzoic acid (TNB)

Transporter of antigen processing (TAP)

Trichloroacetic acid (TCA)

ABSTRACT

CHARACTERIZATION OF FIBROBLASTS WITH A UNIQUE DEFECT IN PROCESSING ANTIGENS WITH DISULFIDE BONDS

Brian J. Merkel, B.A.

A dissertation submitted in partial fulfillment of the requirements for the degree of Doctor of Philosophy at Virginia Commonwealth University.

Virginia Commonwealth University, 1994

Major Director: Kathleen L. McCoy, Ph.D. Associate Professor
Department of Microbiology and Immunology

A Chinese hamster ovary (CHO) fibroblast, transfected with murine major histocompatibility complex (MHC) class II genes, inefficiently stimulated CD4$^+$ Th cells specific for ovalbumin (OVA), hen egg lysozyme (HEL), and pork insulin which contain disulfide bonds. However, the fibroblasts elicited a T cell response to λ-repressor, which lacks disulfide bonds, and efficiently presented synthetic peptides. A somatic cell hybrid WALC, generated by fusing the hamster fibroblast with a murine L cell fibroblast, very efficiently processed OVA and HEL, suggesting that impaired processing was genetically complemented,suggesting that the processing defect is a recessive trait. Three distinct processing phenotypes were observed among twenty-eight hybrid clones analyzed for their ability to process a suboptimal concentration of OVA suggesting that a limited number of genes mediates the defect of WAB4 cells. The hamster fibroblasts were capable of processing two distinct denatured forms of OVA and carboxymethylated HEL either as effectively or more efficiently than a B lymphoma cell. The CHO cells also displayed diminished disulfide reduction of an endocytosed conjugate consisting of ^{125}I-tyramine linked to poly-(D-lysine) through a disulfide spacer compared with that of the cell hybrid, providing direct evidence for defective reductive cleavage by the CHO cells. Diminished aspartic acid-mediated proteolysis of Ag could not account for the phenotype, because cell lysates and separated organelles from the fibroblast possessed higher acidic aspartyl proteolytic activity than lysates and organelles from a B lymphoma cell. The WAB4 cells had normal intracellular levels of cysteine, however they possessed diminished levels of intracellular glutathione (GSH). Buthionine sulfoximine (BSO)-mediated reduction of intracellular levels of GSH decreased the ability of the hybrid line WALC to process HEL. Conversely, treatment of WAB4 cells with N-acetyl cysteine increased their efficiency in the processing of HEL. These findings indicate that the intracellular level of GSH influences the capacity of cells to process antigens with disulfide bonds. Thus, the antigen processing defect exhibited by transfected CHO cells is probably caused by their impaired ability to reduce disulfide bonds which may be related to the diminished intracellular GSH level.

INTRODUCTION

Cell-mediated immunity

Cell-mediated immunity consists of T lymphocytes which are a group of specialized cells capable of recognizing signals in the form of pathogen-derived peptide fragments associated with molecules of the major histocompatibility complex (MHC) that are displayed on the surface of antigen-presenting cells (reviewed in 1). This is the basis for intracellular pathogen detection. The competency with which T cells respond to intracellular pathogens resides in the dual specificity of the T cell receptor (TCR) composed of an $\alpha\beta$ heterodimer, which is distinct from that of B cell antibody-mediated recognition of extracellular intruders.

T cells can be divided into two main subsets based on expression of either CD4 or CD8 accessory molecules (reviewed in 2). Those T cells expressing CD4 are called helper/inducer T cells (T_h) because they typically provide positive signals in the form of secreted lymphokine, which serve to facilitate the differentiation of B cells into antibody-secreting plasma cells. CD4$^+$ T_h cells are specific for or restricted to complexes consisting of MHC class II molecules and antigenic peptide displayed on the surface of antigen-presenting cells (APC). The T_h cells exist in two subsets separated on the basis of differing patterns of lymphokine secretion. The T_h2 subset are those T cells which provide signals, in the form of interleukin-4 and interleukin-5, to B cells. By contrast, the T_h1 subset of cells secrete, among others, interleukin-2 (IL-2) and τ-interferon which culminates in delayed-type hypersensitivity responses. Those T cells expressing CD8 accessory molecules typically function as cytotoxic cells. These activated cells lyse target cells by direct contact. CD8$^+$ T cells are restricted to complexes of MHC class I molecules and stimulatory peptides expressed by APC. What remains controversial is the existence of a distinct lineage of CD8$^+$ T cells called suppressor cells (T_s). It has been appreciated that T cells downregulate the action of B cells and other T cells via lymphokine secretion. However, the inability to generate long-term cloned lines of T_s cells has made the idea of a distinct lineage of suppressor T cells improbable if not impossible .

Molecules of the major histocompatibility complex (MHC)

The MHC was first discovered by immunologists investigating tissue rejection biology (reviewed in 3). For every vertebrate species studied to date, one set of closely linked genes dictates whether or not tissues transplanted between individuals of the same species are rejected (4). The predominant role of a single locus in tissue compatibility led to the terminology of major histocompatibility complex. Genetic factors controlling T cell-dependant immune responsiveness was later mapped to the major histocompatibility locus (5, 6). Clearly, MHC-encoded gene products are involved in a variety of T cell-dependent immune responses including, but not limited to, graft rejection, immune responsiveness, and restriction of immune responses.

Most of the immunologic properties ascribed to MHC are genetically distinguishable and map to different genetic regions. The products encoded by MHC class I and class II genes are highly polymorphic. MHC Class I proteins consist of a 45 kilodalton (kd) MHC-encoded heavy chain and a 12 kd non-MHC encoded beta-2 microglobulin (β_2m). MHC Class II proteins are heterodimers consisting of two MHC-encoded glycoproteins which are noncovalently associated with one another. The α chain has a molecular weight of 33 kd, and the β chain has a molecular weight of 29 kd. MHC class I proteins are present on the surface of nearly all nucleated cells, whereas the class II counterparts are found on a limited number of cell types such as B cells, dendritic cells, and the macrophages (1).

X-ray crystallographic analysis has been conducted on both MHC class I and class II proteins. **Figure 1** shows the peptide-binding groove of the human HLA-A2 class I molecule (7). The distal $\alpha1$ and $\alpha2$ domains of the HLA-A2 class I molecule are arranged into eight antiparallel β-strands as the floor of the groove and two α helices as the sides or walls of the groove. Binding of peptide to MHC class I molecules involves interactions between clustered residues at the ends of the binding groove and the free NH_2 and COOH groups of the peptide (8, 9). These interactions limit the length of peptides in a range of 8-10 amino acid residues capable of binding class I molecules (10). The same view of MHC class II (11) is shown in **Figure 2**. Similar to class I, the binding pocket of MHC class II consists of a floor of eight strands of β-sheet and two helical walls. Although the structure of the groove is extraordinarily similar, the binding of peptides to MHC class II molecules involves main chain atoms in peptides, not the terminal groups. Additionally, the ends of the groove are more open such that peptides can extend beyond the peptide groove (11). The net result of these disparities is that MHC class II peptides are more heterogeneous in size, ranging from 12 to 24 amino acid residues (12-14) and even whole proteins with appropriately extended regions can bind (15),

T cell recognition of peptide and MHC

Antigen recognition by T cells is mediated by the cooperative interactions of the TCR/CD3 complex and the accessory structures CD4 on T_h cells or CD8 on cytotoxic T cells (reviewed in 16). As shown in **Figure 3**, the antigen binding receptor of T cells is a multichain structure comprised of a disulfide-linked α/β heterodimer that is noncovalently associated with the CD3 complex. The CD3 complex is made

Figure 1. Peptide-binding groove of the human HLA-A2 class I molecule. This illustration depicts the top view of the distal portion of the HLA-A2 class I molecule which illustrates the eight strands of antiparalell β-sheet as the floor of the pocket and the two α helical walls. This diagram was prepared from Bjorkman et al (7).

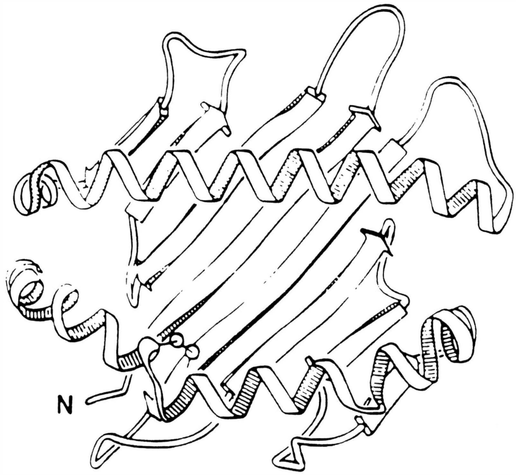
N

Figure 2. Peptide-binding groove of the human HLA-DR1 class II molecule. This representation depicts the α1 and β1 domains of class II molecule. Polymorphic positions are depicted by dark circles. Amino-acid residues are indicated by one letter code. The floor of the class II peptide-binding groove consists of eight antiparallel β-sheet and the walls of the groove consist of two α-helicies. This sketch was obtained by Brown et al (11).

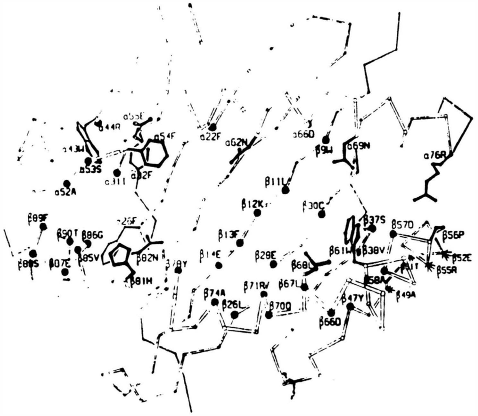
α55E
α44R
α54F
α22F
α62N
α66D
β9W
α69N
α76R
α43W
α53S
α31I
α32F
α52A
β11L
β12K
β30C
β89F
β90T
β86G
α26F
β13F
β37S
β57D
β56P
β88S
β87E
β85V
β82N
β78Y
β14E
β28E
β68L
β61W
β38V
β52E
β81H
β41T
β55R
β58A
β49A
β74A
β71RW
β67L
β26L
β70Q
β47Y
β66D

Figure 3. Schematic illustration of APC-mediated T_h cell activation. The $\alpha\beta$ heterodimer of MHC class II molecules complex with stimulatory peptide fragments and are displayed at the APC surface to $CD4^+$ T_h cells. Recognition of complexes of peptide and MHC class II molecules by T_h cells is mediated by the TCR $\alpha\beta$ heterodimer. CD4 molecule serves as a co-receptor and recognizes a nonpolymorphic region of the MHC class II molecule. Occupancy of the TCR is then converted into a signal that is transduced through the CD3 complex (16).

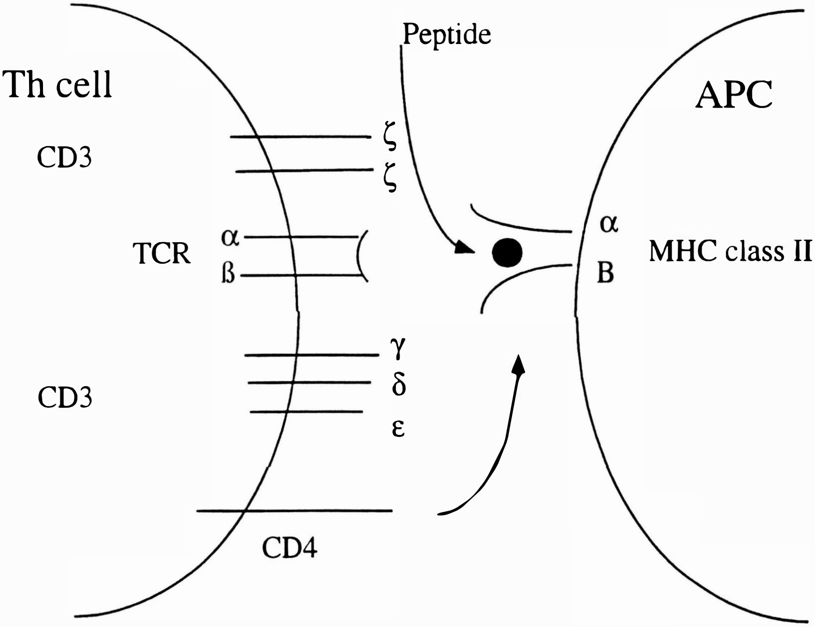
Th cell
Peptide
APC
CD3
ζ
ζ
α
TCR
ß
α
MHC class II
B
γ
δ
ε
CD3
CD4

up of τ dimer, δ, and ϵ, chains and either zeta homodimers or zeta/eta heterodimers.

The TCR has two functions in antigen-induced activation of T cells. The first involves the binding of MHC and peptide by the TCR. The second one is the conversion of the binding event into a signal that is then transduced intracellularly.

CD4 and CD8 molecules serve as co-receptors and bind to nonpolymorphic regions of MHC class II and class I molecules, respectively. The co-receptors enhance the avidity of the T-cell presenting cell interaction and also have an important role in the signal transduction pathway. This series of binding events culminates in the activation of the T cells to become effector cells.

MHC class I presentation

MHC class I proteins bind peptides derived from protein within the cytoplasm whereas class II proteins bind protein fragments obtained within the endocytic route. Evidence supporting the role of MHC class I proteins in the presentation of cytoplasmic peptides was first reported by Townsend et al (17). They identified nuclear viral proteins as the targets of CD8$^+$ cytotoxic cells. In addition, they demonstrated that peptide fragments could substitute for the intact protein. Endogenous synthesis of viral gene products and not their uptake by the endocytic route supported MHC class I-mediated activation of CD8$^+$ T cells (18). Moore et al., and Yewdell et al., (19, 20) demonstrated that MHC class I presentation of peptides derived from exogenous antigens required delivery to the cytoplasm. Finally, the majority of peptides eluted from class I molecules are derived from nuclear and cytoplasmic proteins (21).

A major stride in the understanding of the mechanism of the MHC class I presentation pathway came from studies utilizing mutant cells defective in class I heavy chain-β2m assembly in the endoplasmic reticulum (ER). Addition of peptide to these cells increases their MHC class I expression. The enhanced expression is attributable to peptide stabilization of conformationally correct MHC class I-β_2m complexes (22). A vast amount of evidence suggested that the mutant phenotype is the result of a deficient peptide supply in the ER. Subsequent studies determined that two closely linked genes identified in the MHC class II region of the MHC encoded proteins homologous to transporters in the ATP-binding cassette family (23). These proteins form a heterodimer referred to as transporter associated with antigen processing (TAP) and are resident largely within the ER and cis-Golgi membranes. Transfer of Tap genes into the mutant cells restored MHC class I expression (24). In addition, TAP is responsible for ATP-dependant transport of peptides from the cytoplasm into the ER (25, 26). Therefore, the cytoplasmic pool of peptides is shuttled into the MHC class I containing-lumen of the ER by the TAP heterodimer. Subsequently, the peptides bind MHC class I molecules in the ER, and the is then directed to the cell surface where it can then be recognized by CD8$^+$ cytotoxic T cells.

One obvious question is how are the peptides generated in the cytoplasm? Cytoplasmic protein turnover is mainly handled by proteasomes, multicatalytic protease assemblies (27). Studies have demonstrated that agents capable of inhibiting proteasome function in intact cells greatly reduces the ability of cells to degrade cellular proteins and produce peptides capable of binding class I molecules (28). A subset of proteasome contains two low molecular weight proteins (LMP) encoded by the MHC adjacent to the Tap genes termed LMP-2 and LMP-7. These subunits have been shown to alter cleavage pattern of substrates by the proteasome complex (29, 30). Cells from mice possessing a targeted deletion of the gene encoding Lmp-7 have reduced levels of MHC class I molecules and are deficient in presenting endogenous Ag (31). Addition of peptides to splenocytes deficient in LMP-7 restored normal levels of class I expression. The aforementioned work has come under challenge by data obtained with other cell lines mutated to be deficient in LMP-2 and LMP-7. These cells are capable of processing Ag and delivering peptides to the ER lumen for association with MHC class I molecules (32, 33). The conflicting data may be explained in part, by the distinct methods for the development of these LMP subunit deficient cells. Though the mechanism of MHC class I presentation of endogenously-derived peptides is now fairly well understood, the same does not apply to presentation of peptides derived from exogenous sources.

MHC class II presentation

Although MHC class II molecules are also assembled in the ER, their acquisition of peptides by MHC class II molecules does not occur within the ER but in an acidic compartment. **Figure 4** depicts a model illustrating key aspects of the MHC class II processing pathway. The differences in peptide acquisition by MHC class I and class II molecules is thought to involve disparities in protein assembly. Assembly of MHC class II molecules in the ER involves association of a nonpolymorphic, non-MHC-encoded protein termed invariant chain (Ii) which may serve to prevent binding of endogenously-derived peptides by class II molecules. Ii chain is a type II integral membrane protein (34). A great deal of work has focused on the importance of Ii chain to this particular processing pathway. Although fibroblasts and mutant B cells which express class II molecules but lack invariant chain are capable of activating T cells, the fibroblasts (35, 36) and B cells (37, 38) have impaired assembly, transition and stability of the α and β dimers. It is important to note that (1) MHC class II molecules expressed by these cells resemble the MHC class I molecules devoid of peptide expressed by the cells deficient in TAP.

Another function attributed to Ii chain has been one of maintaining the distinction between the MHC class I and class II presentation pathways. MHC class I molecules have evolved to capture peptides

Figure 4. Model for MHC class II presentation of exogenously-derived peptides. Newly synthesized MHC class II molecules are synthesized in the (RER) where they become associated with the (Ii). The class II/Ii chain complex is shuttled through the Golgi to an endosomal compartment where Ii chain is cleaved by endosomal proteases. Native Ag is taken up at the cell surface and enters the endocytic route. Processing may occur within endosomes and/or lysosomal compartments resulting in peptide generation. The binding of peptide fragments to MHC class II molecules occurs within a specialized compartment called the CPL. Class II/peptide complexes then egress to the plasma membrane they can be recognized by T_h cells.

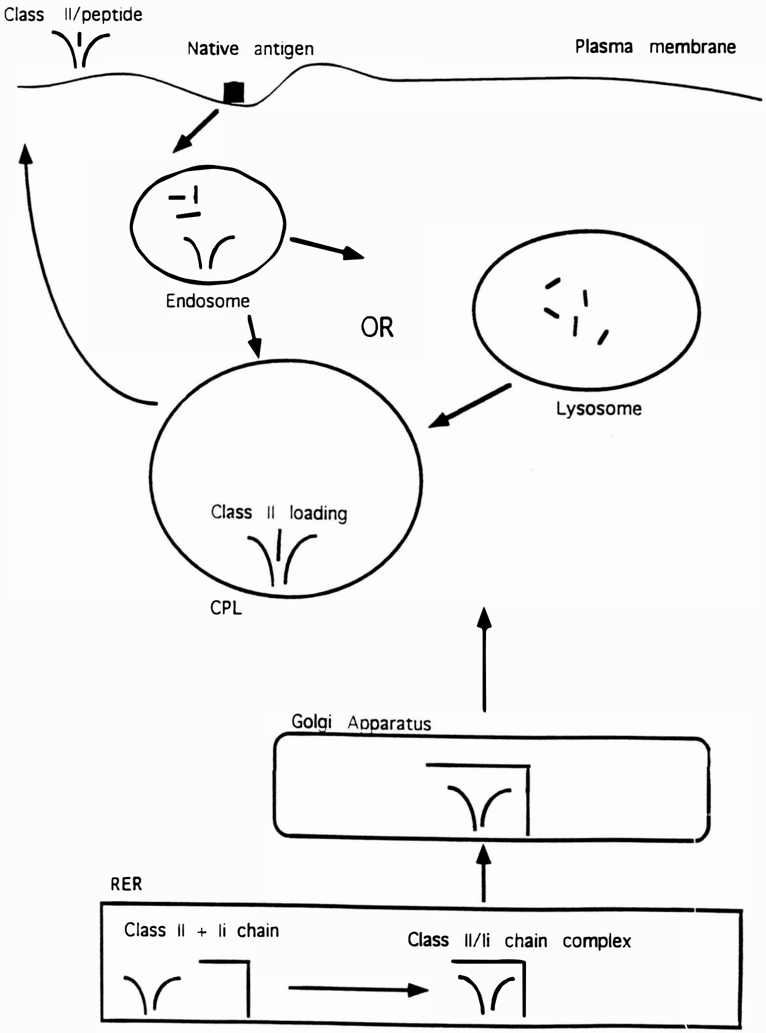
Class II/peptide
Native antigen
Plasma membrane
Endosome
OR
Lysosome
Class II loading
CPL
Golgi Apparatus
RER
Class II + Ii chain
Class II/Ii chain complex

shuttled into the ER from the cytoplasm whereas class II molecules, because they associate with Ii chain in the ER, are unable to bind cytoplasmically-derived peptides and therefore are able to bind peptides generated in the endocytic route (39-41). The segment of Ii chain which binds to class II is called the class II-associated invariant chain peptide containing residues 80-103 (CLIP) region (42). Therefore, class I molecules, synthesized in the ER bind peptides derived from the cytoplasm in contrast to class II molecules, which are associated with CLIP, are unable to access cytoplasmically-derived peptides. Therefore Ii chain maintains the functional distinction between the two classes of molecules.

The processing of exogenously-derived proteins occurs within an acidic compartment. Initial studies involved the use of lysomotropic agents, such as chloroquine, that elevate intracellular pH. Treatment of APC with these agents ablated APC-mediated T cell activation, suggesting that the generation of stimulatory fragments from native proteins occurs within an acidic compartment (43). Though unresolved, it is speculated that signals in the cytoplasmic tail of Ii chain are partly responsible for class II transit to these endocytic compartments (44). Generally, two intracellular acidic compartments are deemed likely candidates as processing compartments. Both the endosomes and lysosomes possess protease activity (45, 46). The heterogeneous endosomes (early vs. late) form following the entry of molecules taken up at the cell surface. Notably, endosomes contain the acid proteases cathepsins B and D (47). Distinct from the endosomes, lysosomes possess a lower pH as well as a variety of other proteases not present in the endosomes (45). For some time, investigators have attempted to determine the relative contribution of endosomes and lysosomes in class II presentation of peptides. Much work has focused on the localization of elements of the processing machinery to one or the other compartment. For example, studies using immunohistochemical staining demonstrated co-localization of MHC class II molecules, Ag, cathepsins B and D within early endosomes (47). Additional support for the contribution of endosomes in antigen processing comes from work utilizing temperature-sensitive mutant cells defective in endosomal acidification. Though the lysosomes remain unaffected in these cells, impaired processing is observed for a variety of Ag (48). Recently, more direct approaches have been developed to assess the contributions of endosomes and lysosomes in processing. These approaches involve the conjugation of antigens to cellular proteins known to traffick to specific intracellular acidic compartments. In one case, transferrin is known to traffick to the endosomes and does not enter the lysosomes (49). Conjugates of transferrin and Ag, which are taken up by receptor-mediated endocytosis are processed more efficiently than unconjugated Ag, which are taken up by fluid-phase pinocytosis. These data suggest that endosomal processing of these Ag results in generation of stimulatory peptides (50). In order to target Ag directly to the lysosomes, Ag have been conjugated to α-2 macroglobulin (51). Findings with these conjugates demonstrate that functional processing of conjugated Ag occurs in the lysosomes. In support of the aforementioned data, Ag targeted to the lysosomes, via acid-resistant liposomes, leads to enhanced processing (52). One interpretation drawn from the antigen targeting data is that different antigens have disparate processing requirements. For example, HEL contains 4 disulfide bonds and may require the more rigorous processing provided by the lysosomes. The lower pH and greater number of acidic proteases found within the lysosomes may be necessary for generation of stimulatory HEL peptides. Additional studies addressing the relative contribution of lysosomal vs. endosomal compartments in Ag processing are needed to better understand the mechanism of the MHC class II processing pathway.

To date, the proteases necessary for peptide generation from exogenous protein sources remains fairly unresolved. The consensus is that acidic proteases or cathepsins resident in endosomes and lysosomes are responsible for proteolytic cleavage. Much of the studies assessing the role of cathepsins in processing exogenous Ag has involved class-specific protease inhibitors. Depending on the Ag and T cell, much of the work utilizing these inhibitors suggests the importance of cysteine and/or aspartyl proteases in peptide generation. For example, the aspartyl proteases cathepsins E and D have been shown to be important for the generation of stimulatory peptide fragments recognized by T_h cell clones specific for ovalbumin (53-55).

So, once the peptides are generated, where do they associate with MHC class II molecules? Recently, four groups of investigators have identified MHC peptide-loading compartments in B cells referred to as the compartment for peptide loading CPL (56-59). Two of the groups used sub-cellular fractionation experiments utilizing free-flow electrophoresis (56) or density gradient electrophoresis (57) to distinguish the MHC class II-containing compartments from early and late endosomes. These CPL compartments are distinct from endosomes and lysosomes by their subcellular fractionation behavior, their low or no expression of endosomal and lysosomal markers, and their low accessibility to fluid-phase markers. They are distinct from lysosomes in that they fail to express appreciable levels of lysosomal membrane proteins. Perhaps, Clip is removed from MHC class II molecules in this compartment where peptide loading is thought to occur.

The recent description of another set of mutant APC has greatly assisted the characterization of Ag processing pathways, particularly for the MHC class I processing pathway (60, 61). In the case of exogenous Ag, a panel of mutant cells has been described exhibiting impaired presentation of native Ag, but not of peptides, to MHC class II-restricted T cells (62, 63). Although their MHC class II genes themselves are normal, the class II molecules have abnormal conformation. The Ag processing defect has been attributed to the deletion of the Dma or Dmb genes within the MHC locus (64, 65). Sequence analysis of the genes has shown that DMA and DMB share homology with MHC class II genes, but lack extensive polymorphism. Cells deficient in DM expression fail to express a normal repertoire of MHC-class II peptide complexes. Transfection of the mutant cells with the Dm genes restores normal Ag processing (64, 65). In view of these observations, a variety of models for DM function have been proposed. One possible function of the DM gene products are to serve as a chaperone for class II molecules to a peptide loading compartment such as the CPL. A second possibility is that DM removes CLIP peptides from MHC class II molecules, thereby, allowing the association of exogenously-derived peptides with MHC class II molecules.

Lysosomal reductive cleavage mechanism

The molecular structure of immunogenic Ag greatly varies in terms of size, charge, number of subunits, and post-translational modifications. Yet, the peptides from diverse Ag must retain the ability to bind MHC class II molecules. Given the diversity of Ag and the constraint for antigenicity, the notion that the steps during processing differs among individual Ag is a logical possibility.

An increasing body of evidence supports the hypothesis that Ag conformation dictates the processing stringency required to yield immunogenic peptides from the native protein. In some instances, prior reduction and unfolding of particular Ag greatly enhances presentation efficiency (66-68). Once denatured, these Ag do not need to be proteolytically cleaved. In contrast, other Ag require the additional step of cleavage. Even in this situation, denaturation of the Ag may influence the efficiency of processing. Currently, the intracellular location and mechanism of disulfide bond cleavage of Ag remain somewhat unresolved.

A recent model illustrating the key components of lysosomal reductive cleavage in fibroblasts is shown in **Figure 5**. Upon entering the cytosol, cystine is reduced by reduced glutathione (GSH) to form cysteine. Cysteine can then be transported into the lysosome via a cysteine-specific lysosomal transport system. Once inside the lysosomes, cysteine can react with protein disulfide bridges (69) facilitating disulfide cleavage. Currently, the contribution of this reductive mechanism to Ag processing remains largely undefined.

Rationale and objectives

Considering both the importance and lack of understanding of the MHC class II processing pathway, the focus of this work was to elucidate the mechanism by which MHC class II processing generates peptides capable of being recognized by CD4$^+$ T$_h$ cells. The overall approach was to study an APC clone defective along this pathway. In a previous study, temperature-sensitive mutant cells were used that expressed defective endosomal acidification at the nonpermissive temperature (48). The mutant and wild-type parental Chinese hamster ovary cells (CHO) were transfected with murine MHC class II genes to convert them to APC. The wild-type cells effectively process native Ag including pigeon cytochrome c and Staphylococcal nuclease (48). Surprisingly, this is not the case for all Ag.

A series of studies were designed to describe the genetic basis for the defect. These approaches consisted of genetic complementation, karyotypic analysis, and characterization of a panel of hybrid clones generated in complementation experiments which are both competent and incompetent APC.

A second cluster of experiments were designed to determine what step in antigen presentation was impaired. Various parameters were assessed including the ability of the defective cells to present stimulatory peptides, the importance of antigen structure such as glycosylation and

Figure 5. Lysosomal reductive cleavage mechanism.
Once inside the cytoplasm, cystine is converted into cysteine via GSH-mediated reduction. Cysteine is then transported across the lysosomal membrane via a cysteine-specific lysosomal transporter. Cysteine can react with protein disulfide bridges in a two-step exchange reaction (69). The disulfide cleavage produces free sulfhydryls in the protein and cystine is produced. The cystine exits the lysosomes and is again available for reduction by GSH.

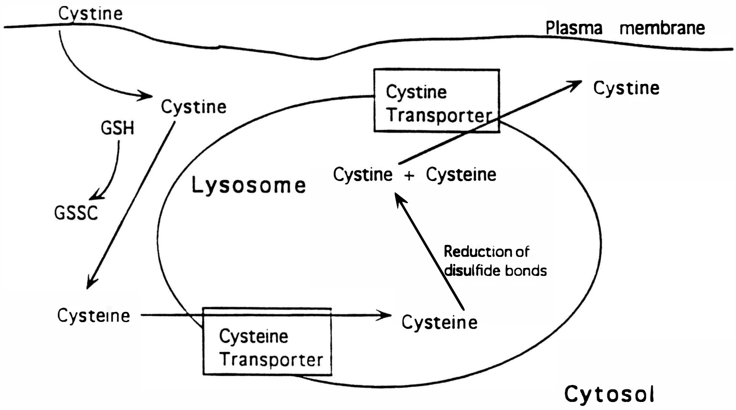
Cystine
Plasma membrane
Cystine
GSH
GSSC
Cystine Transporter
Cystine
Lysosome
Cystine + Cysteine
Reduction of disulfide bonds
Cysteine
Cysteine
Cysteine Transporter
Cytosol

presence of disulfide bonds, and the ability of our defective cell to cleave disulfide bonds.

The third set of related studies were designed to elucidate the mechanism of the defect of these cells. Overall, these experiments examined the integrity of lysosomes to reduce disulfide bonds. The individual components of the lysosomal mechanism were assessed including intracellular levels of glutathione and cysteine as well as the proficiency of an intracellular cysteine transporter. Other experiments examined the effect of increasing intracellular levels of glutathione on the ability of our defective clone to process antigens. Similar experiments were designed to determine the effect of decreasing intracellular levels of glutathione on antigen processing by the hybrid cells which are competent APC.

MATERIALS AND METHODS

1. Cell lines.

The derivation and specificities of ovalbumin (OVA)-specific, I-A^d-restricted T_h cell hybridoma 3DO-54.8, the pigeon cytochrome c-specific, I-E^k-restricted T_h cell hybridoma 2B4 and the λ-repressor-specific, I-A^d-restricted T_h cell hybridoma 7B7.3 were previously described and were kindly provided by Dr. Ronald Schwartz (National Institutes of Health, Bethesda, MD) (70, 71). The hen egg lysozyme (HEL)-specific, I-A^d-restricted T_h cell hybridoma 9.30.B2 was kindly provided by Dr. Eli Sercarz (University of California, Los Angeles, CA) and recognizes the peptide fragment 11-25. The generation of pork insulin-specific, I-A^d-restricted Th cell hybridoma Pd.2.30 was previously described (72) and was kindly provided by Dr. Peter Jensen (Emory University, Atlanta, GA). The generation of the B lymphoma cells TA3 and LK35.2, and the CHO transfectant WAB4 expressing I-A^d MHC class II molecules from the wild-type parental (WTB) CHO cell used as APC were previously published (48, 73, 74) and were kindly provided by Dr. Ronald Schwartz. The mouse fibroblast transfectant L cells (DECK Hi7) expressing I-E^k molecules were kindly provided by Dr. Ronald Germain (National Institutes of Health). The derivation of the IL-2-dependant cell line CTLL-2 was previously published (75) and was obtained from American Tissue Culture Collection (Rockville, MD).

2. Ag and mAb.

OVA, HEL, carboxymethylated HEL (CM-HEL), and pork insulin were purchased from Sigma Chemical Co (St. Louis, MO). λ-repressor (1-102) and its $\text{peptide}_{12\text{-}26}$ were supplied by Dr. Ronald Schwartz. A synthetic peptide of $OVA_{323-339}$ was produced and purified by the protein core facility (Virginia Commonwealth University, Richmond, VA). The synthetic peptide of HEL_{11-25} was purchased from Chiron Mimotopes (Raleigh, NC). The monoclonal antibodies (mAb) were purified by protein-A affinity column chromatography from cell-free culture supernatants of MKD6 (anti-I-A^d; 76), Y-17 (anti-I-E^k; 77), MAR 18.5 (anti-rat κ chain; 79). These cells along with 15-1-5-P (anti-K^kD^k; 78) were obtained from ATCC. MKD6 and MAR18.5 were conjugated with fluorescein isothiocyanate (FITC) isomer I (Molecular Probes, Eugene OR) and Y-17 was biotinylated after extensive dialysis in 0.05 M borate-0.1 M NaCl buffer at pH 9.5. FITC (100 μg) or N-hydroxy succinimido-biotin at 100 mg per antibody was added, mixed and incubated at room temperature for 2-3 hours (h). Conjugated antibody was then dialyzed in 0.05 M Tris-0.15 M NaCl buffer containing 0.2 % NaN_3 at pH 7.5. Conjugated antibody was then centrifuged at 10,000 rpm for 5 minutes in Eppendorf microfuge to clear aggregated material. The protein concentration was determined by the absorbance at 280 nm using the extinction coefficient of 1.38 (ϵmg/ml). The amount of FITC conjugated to protein was determined by absorbance at 495 nm. The ratio of FITC/protein was calculated and was ≥ 2.0. The specificity of the Ii chain-specific mAb In-1 was previously described (80) and was kindly provided by Dr. Ronald Germain.

3. T cell stimulation assay.

IL-2 secretion by Th_1 cells was used to determine APC effectiveness. The principle of the assay involves measuring proliferation of the cell line CTLL which depends on IL-2 for growth. The level of incorporation of radiolabeled nucleotides by CTLL on a logarithmic scale is linearly related to the quantity of IL-2 in the culture supernatants. T_h cells at 3×10^4 were cultured with 5×10^4 APC with or without various concentrations of Ag in 96-well flat bottom microtiter plates (Costar, Kingsbridge, MA) for 24 h. Culture supernatants were harvested and assayed in duplicate for the presence of IL-2 by incubating the IL-2-

dependant cell line CTLL-2 with 25% supernatants for 18 h. The wells were pulsed with 1 μCi of [^{3}H]-thymidine (Amersham, Arlington Heights, IL) and harvested after another 6 h. Radiolabeled incorporation was quantitated by liquid scintillation counting. In some experiments, APC were fixed with 0.5% paraformaldehyde prior to culture as previously described (48).

4. Somatic cell hybrid generation.

WAB4 (G418-sensitive) and DCEK Hi7 L cells (mycophenolic acid-sensitive) expressing murine I-A^d and I-E^k MHC class II gene products, respectively, were fused via 1 g/ml polyethylene glycol (PEG) treatment. Hybrids were isolated by a double drug selection protocol with 6 μg/ml mycophenolic acid and 200 μg/ml gentamicin (G418). The surviving cells were analyzed for surface expression of I-A^d and I-E^k MHC class II molecules by two-color flow cytometric analysis using FITC-MKD6 and biotinylated Y-17 (see **MATERIALS AND METHODS #6**).

5. Karyotypic analysis.

Karyotypic analysis of WAB4 DCEK Hi7 and one hybrid cell line of uncloned cells, WALC, was performed by Genetic Research Inc. (Durham, NC).

6. Cloning of hybrid cells.

The hybrid cells were cloned by colony lift. Hybrid cells were placed (200 cells/plate) in 100 mm petri dishes (Costar). Individual colonies were removed with Whatman's filter paper # 2 (Baxter, Columbia, MD) and placed in 24-well plates (Costar). Cloned population of cells were then expanded and assayed for dual expression of I-A^d and I-E^k MHC class II molecules (**see MATERIALS AND METHODS #7**) and for ability to process a suboptimal concentration of OVA (**MATERIALS AND METHODS #3**).

7. Immunofluorescence staining and flow cytometry.

Cells were stained as described elsewhere (50). a. Class II surface labeling. The expression of I-A^d molecules was detected by incubating cells with FITC-MKD6. Background controls were cells incubated with unlabelled MKD6 supernatant, followed by FITC-MKD6. For I-E^k expression, cells were stained with biotinylated Y-17, followed by phycoerythrin-avidin. Non-specific fluorescence was determined by incubating cells with phycoerythrin-avidin only. b. Class I surface labeling. The expression of H-$2K^kD^k$ MHC class I molecules was determined by incubating cells with 15-1-5P (78), followed by $F(ab)'_2$ fragment of FITC-labeled goat anti-mouse IgG antibodies (Organon Teknika Corp., Durham, NC). Background levels were determined by incubating cells only with the secondary antibodies. c. Cytoplasmic staining of Ii chain. Intracellular Ii expression was determined by first permeabilizing the cells with 0.1% saponin (Sigma) in phosphate buffered saline (PBS). The cells were fixed with 10% formalin for 10-14 minutes at room temperature followed by 30 min incubations with In-1 and then FITC-MAR 18.5 at room temperature. Following fixation and incubations, cells were washed with 0.1% saponin in PBS. Fluorescence intensity was measured by flow cytometry utilizing a Becton Dickinson FACScan (San Jose, CA) equipped with a 15 mW 488 nm argon laser. Data were collected on 10,000 cells with logarithmic amplification and analyzed by a Hewlett Packard series 300 computer (Portland, OR).

8. Aspartic acid protease assay.

The level of acidic aspartyl proteolytic activity in cell lysates and isolated organelles was measured as described (81). Cell lysates were prepared from WAB4 and TA3 cells at 1.0 X 10^8/ml in 0.75% Triton X-100 lysis buffer. Organelles were isolated from 5 X 10^7 cells, which were disrupted by N_2 cavitation, by density centrifugation through a 23% Percoll-sucrose gradient of 17.5 ml as described (50). Density marker beads (Sigma) were used to estimate the density profile of the gradient. One-ml fractions were collected from the top of the gradient. Lysosomal β-galactosidase activity in the fractions was quantitated as previously described (50), and the results are expressed in arbitrary fluorescence units. Total protein concentration was determined by bicinchoninic acid assay (Pierce Chemical Co., Rockford, IL). Samples in duplicate were assayed for proteolytic cleavage of 8% hemoglobin in a 1 M sodium acetate buffer at pH 4.5 with or without the aspartyl protease inhibitor 10 μg/ml pepstatin A (Sigma) for 150 min at 37°C. The assay is done under acidic conditions to preclude involvement of other non-acidic proteases in hemoglobin cleavage. Aspartyl protease-mediated degradation of hemoglobin was determined by measuring the absorbance at 550 nm using a background control which lacked cell samples. Aspartic acid proteolytic activity was determined by subtracting the absorbance in samples containing pepstatin A (non-aspartyl protease activity) from the values of samples lacking pepstatin A (total aspartyl protease activity). One unit of enzymatic activity is a net absorbance of 1.0. Activity is expressed as units/mg protein ± SD to compensate for any difference in cell number.

9. Endoglycosidase H removal of carbohydrate residues

OVA (45 mg) was suspended in 2.25 ml of 0.05 M citrate buffer at pH 5.0 with (treated) or without (untreated) 450 milliunits of recombinant Endoglycosidase-H (Boehringer mannheim, Indianapolis, IN). The incubation was allowed to proceed for 20 h in a 37° C water bath. The reaction was neutralized by passing the OVA preparations over a P6DG desalting column.

10. Separation of glycosylated and unglycosylated OVA

Glycosylated and unglycosylated OVA was separated by passage over an affinity chromatography column consisting of concanavalin A (Con A) bound to a sepharose matrix (Sigma). OVA in the void volume was considered as unglycosylated. The glycosylated OVA was eluted from the affinity column with 0.1 M alpha-methyl mannoside (Sigma). Protein concentration was determined by the absorbance at 280 nm with the extinction coefficient 0.485 (ϵ mg/ml). Purity of the glycosylated and unglycosylated OVA preparations were assessed by 7.5% SDS-PAGE.

11. Enzyme-linked immunoabsorbant assay (ELISA) of glycosylated OVA

Degree of glycosylation of OVA preparations was determined by ELISA. ELISA plates were coated in triplicate with either 100 μg/ml of unglycosylated or glycosylated samples from both ENDO-H treated or untreated OVA along with parallel wells of OVA standard ranging in concentration from 100 μg/ml to 0.78 μg/ml overnight at room temperature. The wells were then washed with 0.05 % Triton X-100 in PBS. To decrease nonspecific binding, wells were coated for 30 min with 0.1% gelating in PBS. The wells were then washed with 0.05 % Triton X-100 followed by incubation of wells with 2.5 μg/ml Con A-biotin for 1 h which would recognize α-mannosyl residues coated on the ELISA plates. Wells were washed with 0.05 % Triton X-100 followed by incubation with 0.0625 μg/ml avidin-peroxidase for 1 h. Wells were washed with 0.05 % Triton X-100 followed by incubation with 2,2'-azino-bis(3-ethylbenzthiazoline) ABTS (Kirkegard and Perry Labs Inc. Gaithersburg, MD) peroxidase substrate for 6 min. Potassium fluoride (KF) was added to terminate the reaction. Absorbance was determined at 405λ using a Molecular Devices Corporation ELISA reader (Palo Alto, CA) equipped with Softmax software. Data are presented as optical density units with having blank, lacking sample, subtracted. Preparations of unglycosylated OVA (100μg/ml) possessing levels of glycosylation similar to OVA standard at 0.78 μg/ml were considered sufficiently unglycosylated and were tested for potency in our APC-mediated T cell stimulation assay (**see MATERIALS AND METHODS #3**). To test for possible Con A contamination, OVA preparations generated with the con A sepharose column were tested for T cell mitogen activity by incorporating these preparations in the T cell assay. Activation of the T_h cell hybridoma 2B4, which is specific for pigeon cytochrome c, in the presence of OVA, was the basis for detecting Con A contamination.

12. Disulfide bond reduction of Ag.

OVA at 15 mg/ml was denatured and reduced by incubation with 8 M urea and 0.2 M 2-mercapatoethanol under N_2 atmosphere for 12 h at room temperature as previously described (82, 83). For carboxymethylated OVA (CM-OVA), 0.3 M iodoacetic acid (Sigma) was incubated with Ag for 2 h at room temperature under N_2 atmosphere. To generate a non-carboxymethylated OVA (D-OVA), 0.1 M Tris buffer was added after reduction. The proteins were extensively dialyzed before use in 0.1 M Na_2HPO_4. Free sulfhydryl content was determined before and after reduction, and after carboxymethylation by Ellman's assay (Pierce). The principle of the assay involves the specificity of 5,5'-dithiobis-(nitrobenzoic) acid (DTNB) (Ellman's reagent) for free sulfhydryl groups which generates a mixed disulfide and 2-nitro-5-thiobenzoic acid (TNB). Therefore sulfhydryl groups are quantitated by comparing an unknown against a standard curve containing cysteine. By this criterion, all disulfide bonds were reduced by 2-mercaptoethanol, and all free sulfhydryl groups were derivatized by iodoacetic acid. No protein fragmentation was detected by 12% SDS-PAGE.

13. Circular dichroism.

Measurements of circular dichroism on native OVA, D-OVA, CM-OVA, HEL, and CM-HEL were quantitated by a Jasco model 500 spectropolarimeter (Japan Spectroscopic Co., Tokyo, Japan). Helical character was determined by comparing millidegree values at 220 nm for each protein.

14. Cellular disulfide reductive function.

Cells at 8 X 10^5-1 X 10^6 were cultured in 6-well culture dishes in duplicate, one day prior to incubation with the ^{125}I-tyramine linked to poly-(D-Lysine) through a disulfide spacer conjugate (^{125}I-tyn-SS-PDL). The following day cultures were washed with cold serum-free EMEM containing 25 mM HEPES and incubated for 60 min at 0°C in the serum-free medium containing ^{125}I-tyn-SS-PDL (1μg/ml, 2 X 10 ^{5} cpm per well) to label the surface of the cells. Conjugate probe was prepared as previously described (84). The cells were washed twice and incubated in prewarmed serum-free medium at 37°C up to 2 h in 30 min intervals. All subsequent steps were carried out as previously described (80). N-ethylmaleimide (20 mM) (NEM) was added to the cultures. Cell lysates were prepared in 0.1% Triton X-100 and precipitated with 7.5% trichloroacetic acid (TCA). The radioactivity in the supernatant and pellet was determined by a gamma counter. The quantity of TCA-soluble radioactivity was a measure of the reduction of the conjugate.

15. Intracellular levels of cysteine and glutathione

Cells were washed twice in PBS and suspended in 2.5% sulfosalicylic acid (Sigma) at a concentration of 1 X 10^7 cells/0.4 ml. Cell lysis was allowed to proceed for 20 min on ice. Precipitated protein and supernatants were separated via centrifugation. Protein pellets were suspended in an equal volume of neutralizing 2 N NaOH. Protein concentration of suspended protein pellets was determined by bicinchoninic (BCA) assay (Pierce). a. Acid-soluble cysteine was measured as described (85). An equal volume of acid-soluble supernatant was added to acid ninhydrin which consisted of 250 mg ninhydrin in a mixture of 6 ml acetic acid and 4 ml concentrated hydrochloric acid. The acid ninhydrin/supernatant mixture was heated for 10 minutes at 100° C. Absorbance was measured at 560 nm against a blank consisting of acid ninhydrin reagent alone. Cellular proteins and not thiols like cysteine and glutathione will be precipitated with 2.5 % sulfosalicylic acid. The specificity of ninhydrin for cysteine in the soluble fraction is due to the wavelength (550 nm) used to measure absorbance and the pH of the assay mixture. b. Acid-soluble-glutathione was measured as described (86). The standard assay system for glutathione consisted of 0.6 µmole Ellman's reagent DTNB (Pierce), acid-soluble cell lysate or 10-50 ng oxidized glutathione (GSSG) standard (Sigma), 10 µg glutathione reductase, and the glutathione reductase cofactor nicotinamide adenine dinucleotide phosphate (NADPH). Oxidized glutathione in either the form of the standard or in cell lysates is reduced by glutathione reductase to reduced glutathione. The assay actually measures the reduced glutathione-mediated reduction of DTNB to NTA over time. The rate of reaction is expressed as the change in absorbency per 3 min at 412 nm against a blank consisting of 2.5% sulfosalicylic acid only. Reaction is initiated by the addition of NADPH which results in rate of color development at 412 nm that is linear beyond 6 minutes.

16. Cysteine transporter activity

Cysteine transporter activity was determined according to the method described (87). Cells (20×10^6) were washed twice in PBS. Cells were suspended in 0.1% glucose in (hank's balanced salt solution) HBSS followed by the addition of 30 μCi of [^{35}S]L-cystine (Dupont, Wilmington, DE). Incubation was allowed to proceed for 15 minutes at 37° C. The cells were then extensively washed with PBS to remove excess [^{35}]-L-cystine. Cells were then suspended in PBS containing 10 mM NEM and centrifuged. Pellets were suspended in lysis buffer consisting of 0.25 M sucrose and 10 mM NEM. The cells were then subjected to N_2 cavitation for 20 min at 4°C at 250 psi. The cell lysates were collected and centrifuged at 1,500 x g for 10 minutes to obtain the nuclear and postnuclear fractions. To obtain the granular pellet, the postnuclear supernatant was subjected to ultracentrifugation at 20,000 x g. The resulting supernatant represented the cytosolic portion of the cells. Aliquots of the postnuclear supernatant (1,500 x g), the granular pellet (20,000 x g), and the cytosol (20,000 x g supernatant) were assayed for radioactivity and β-galactosidase activity. β-galactosidase activity was used to account for differences in lysosomal content among various cell types. The remainder of the granular pellet was placed on a 23 % Percoll-sucrose gradient and fractionated as described above (**see MATERIALS AND METHODS #8**). The distribution of cysteine transporter activity was determined by determining the radioactivity in gradient fractions.

17. Inhibition of glutathione synthesis

Inhibition of de novo synthesis of GSH is mediated by L-(S,R)-buthione sulfoximine (BSO) (Sigma) which inhibits the activity of τ-glutamyl synthetase. τ-glutamyl synthetase is necessary for the generation of τ-glutamyl-cysteine, a precursor to GSH (89). Therefore, hybrid cells described in **#4 of the MATERIALS AND METHODS** were washed into RPMI medium with or without 160 μM (BSO) (Sigma) and were allowed to incubate overnight at 37°C in 6-well plates (Costar) at 1 X 10^6 cells/well. The following morning, hybrids were pulsed for 5 h with a suboptimal concentration of HEL or medium alone. In the presence of 160 μM BSO. Untreated cells were pulsed with Ag or medium alone lacking BSO. Concomitant with antigen pulse, cell lysates of hybrids incubated with or without BSO were generated to determine intracellular glutathione levels at the time of Ag pulse. The hybrids were trypsinized, harvested, washed free of BSO and placed in 96-well plates. Following addition of 9.30.B2 T_h cells, APC-mediated T cell activation (**see MATERIALS AND METHODS #3**) was allowed to proceed for 24 h.

18. N-acetyl cysteine treatment of WAB4 cells

WAB4 cells at 0.5 X 10^6 were washed in medium with or without 1.0 mM N-acetyl cysteine (Sigma) in an attempt to increase GSH levels. The rate limiting step of GSH synthesis is the generation of τ-glutamyl-cysteine from its constituent amino acids. Prevention of limiting amounts of cysteine in the GSH metabolic pathway is facilitated by treatment of cells with N-acetyl cysteine (89). After 9 h, the medium was replenished with N-acetyl cysteine. Following a 12 h incubation, WAB4 cells were pulsed for 5 h with a suboptimal concentration of HEL. Concomitant to Ag pulse, wells of treated and untreated WAB4 were harvested in order to generate cell lysates which were then measured for intracellular levels of glutathione. Following Ag pulse, WAB4 were washed free of drug and co-cultured with the T cells as described in the **MATERIALS AND METHODS #3**.

RESULTS

1. Limited defect of WAB4 cells in Ag processing

Considering both the lack of understanding and the importance of the MHC class II processing pathway, the focus of this work was to elucidate the mechanism by which MHC class II processing generates peptides capable of being recognized by CD4$^+$ T$_h$ cells. The overall approach was to study an APC clone defective along this pathway. In a previous study, temperature-sensitive mutant cells were used that expressed defective endosomal acidification at the nonpermissive temperature (48). The mutant and wild-type parental Chinese hamster ovary cells (CHO) were transfected with murine MHC class II genes to convert them to APC. To study the mechanism and regulation of the MHC class II processing pathway, we assessed the competency of the transfected CHO cells (WAB4) for each of the key steps for the MHC class II processing pathway. The ability of the CHO fibroblast I-A^d transfectant WAB4 to process a panel of distinct native Ag was investigated. The efficiency of Ag processing was assessed by examining the ability of the cells to activate T$_h$ cells to secrete IL-2 in response to Ag. As shown in **Figure 6A**, the pork insulin-specific, I-A^d-restricted T$_h$ cell hybridoma Pd.2.30 secreted virtually no IL-2, when WAB4 cells were the source of APC. In contrast, a response by these T cells was readily observed with the B lymphoma cell TA3 as the APC. Similar results were obtained with another T cell hybridoma specific for insulin (data not shown). These findings were not unique to pork insulin. WAB4 cells were also very poor in activating the HEL-specific T cell 9.30.B2 (**Figure 6B**). The extremely low response at 189 μM HEL elicited by WAB4 cells was comparable to the level

Figure 6. T cells specific for Ag possessing disulfide bonds are not activated by WAB4 cells. T cells were stimulated with or without various concentrations of native Ag in μM, and with CHO transfectant WAB4 cells (open circles) or B lymphoma cells (closed circles) as the APC. Culture supernatants were collected after 24 h and assayed for IL-2 as described in the **MATERIALS AND METHODS**. Values represent mean cpm of experimental cultures from 25% culture supernatants in the IL-2 assay ± SD. Each experiment shown is representative of three. *(A)* Response of pork insulin-specific, I-A^d-restricted Th cell hybridoma Pd.2.30. The medium controls for WAB4 and TA3 cells were 3,195 ± 654 and 2,510 ± 528 cpm, respectively. *(B)* Response of HEL-specific, I-A^d-restricted Th cell hybridoma 9.30.B2. The medium controls for WAB4 and TA3 cells were 2,884 ± 670 and 1,748 ± 1113 cpm, respectively. *(C)* Response of OVA-specific, I-A^d-restricted Th cell hybridoma 3DO-54.8. The medium controls for WAB4 and TA3 cells were 1,159 ± 61 and 687 ± 184 cpm, respectively. *(D)* Response of λ-repressor-specific, I-A^d-restricted T cell hybridoma 7B7.3. The medium controls for WAB4 and LK35.2 cells were 3,956 ± 1,208 and 4,125 ± 389 cpm, respectively.

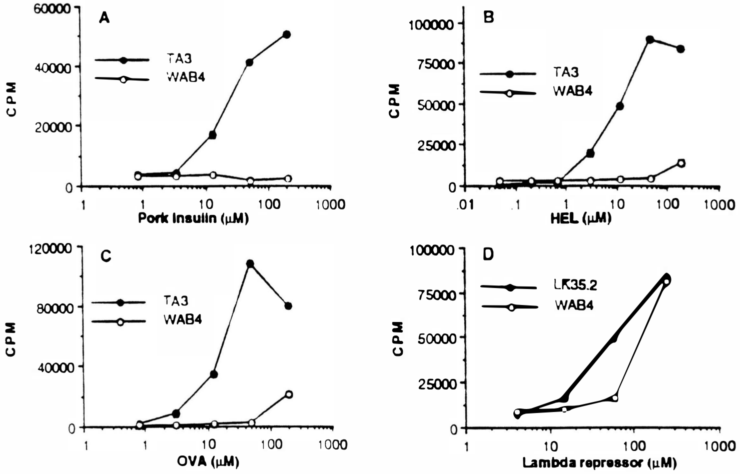
A
60000
40000
20000
0
CPM
TA3
WAB4
1
1
10
100
1000
Pork insulin (μM)
B
100000
75000
50000
25000
0
CPM
TA3
WAB4
.01
.1
1
10
100
1000
HEL (μM)
C
120000
80000
40000
0
CPM
TA3
WAB4
1
1
10
100
1000
OVA (μM)
D
100000
75000
50000
25000
0
CPM
LK35.2
WAB4
1
10
100
1000
Lambda repressor (μM)

of activationproduced at approximately 100-fold less Ag when TA3 cells were the APC. Again, analogous results were obtained with OVA (**Figure 6C**). WAB4 cells induced a low response only at the highest concentration of OVA.

However, different findings were observed with a fourth Ag. WAB4 cells in the presence of intact Ag competently activated the λ-repressor-specific hybridoma 7B7.3 to secrete IL-2 (**Figure 6D**). This finding with λ-repressor agrees with a previous report that CHO transfectants efficiently stimulate Th cell responses to pigeon cytochrome c and Staphylococcal nuclease (48). Thus, the ability of WAB4 cells to activate T cells was limited to certain Ag.

2. **WAB4 cells present peptides**

To distinguish between a problem in Ag presentation or processing, T cell responses to peptides, which do not require processing, were examined. WAB4 cells were fully capable of presenting the synthetic peptide of λ-repressor$_{12-26}$ to the T cells in comparison to the B lymphoma cells (**Figure 7A**). Additionally, WAB4 cells were more efficient than TA3 cells in stimulating the T cells with the synthetic OVA peptide$_{323-339}$ (**Figure 7B**). Similarly, WAB4 cells also were more effective than TA3 cells at eliciting a response by T cells specific for the synthetic peptide of HEL$_{11-25}$ (**Figure 7C**). Thus, the defect appears to involve Ag processing, not peptide presentation.

3. **The defect of WAB4 cells is recessive**

To examine whether the processing defect expressed by WAB4 cells was a dominant or recessive trait, genetic complementation was performed. Somatic cell hybrids were generated by fusing WAB4 cells with murine DCEK Hi7 L cell fibroblast that had been transfected with MHC class II I-E^k genes. In contrast to WAB4 cells, L cell transfectants are capable of processing native OVA (88). The hybrid WALC cell line, unlike WAB4 cells, (**Figure 8A andB**) were able to process efficiently both native OVA

Figure 7. Normal peptide presentation by WAB4 cells. Secretion of IL-2 by T cells was measured (see Fig. 1 legend). *(A)* WAB4 cells (open circles) and B lymphoma LK35.2 cells (closed circles) as the APC were incubated with 7B7.3 and the peptide$_{12\text{-}26}$ of λ-repressor at the indicated concentrations in μM. The results are from the same experiment as in Fig. 1*D*. (see Fig. 1 legend for medium controls). The experiment is representative of three. *(B)* Stimulation of 3DO-54.8 with a synthetic peptide of OVA$_{323\text{-}339}$ at the indicated concentrations in μM using WAB4 cells (open circles) and TA3 cells (closed circles) as the APC. The medium controls for WAB4 cells and TA3 cells were 2,164 ± 358 and 1,658 ± 141 cpm, respectively. The experiment is representative of three. *(C)* Stimulation of 9.30.B2 to peptide$_{11\text{-}25}$ of HEL at the indicated concentrations in μM using WAB4 cells (open circles) and TA3 cells (closed circles) as the APC. The medium controls for WAB4 cells and TA3 cells were 1135 ± 128 and 1731 ± 416, respectively. Experiment is representative of two.

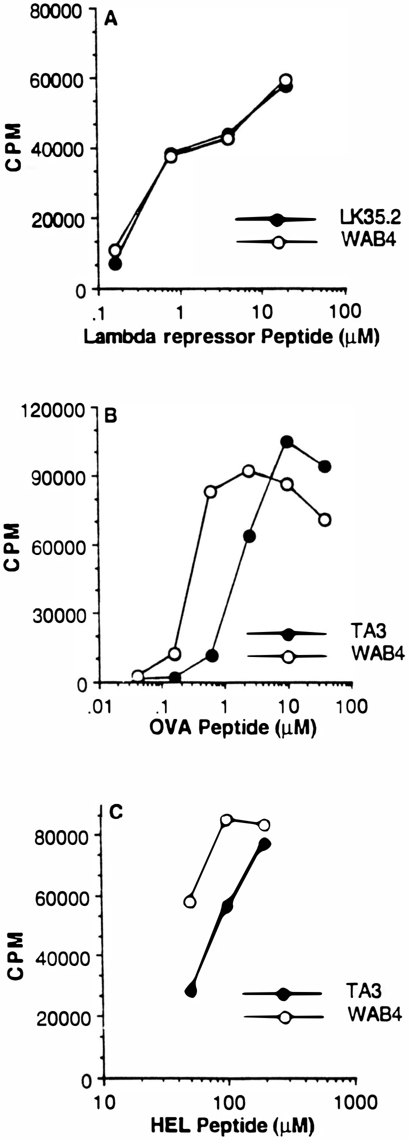
A
80000
60000
40000
20000
0
CPM
LK35.2
WAB4
.1
1
10
100
Lambda repressor Peptide (μM)
B
120000
90000
60000
30000
0
CPM
TA3
WAB4
.01
.1
1
10
100
OVA Peptide (μM)
C
80000
60000
40000
20000
0
CPM
TA3
WAB4
10
100
1000
HEL Peptide (μM)

Figure 8. Rescue of Ag processing by genetic complementation. WAB4 cells (open circles) and the cell hybrid WALC (closed circles) were the APC (see Fig. 1 legend). Values are the mean cpm of experimental cultures ± SD. Both experiments are representative of three. *(A)* Response of 3DO-54.8 to native OVA. The medium controls for WAB4 and WALC cells were 1,159 ± 43 and 818 ± 113 cpm, respectively. *(B)* Response of 9.30.B2 to native HEL. The medium controls for WAB4 and WALC cells were 1,500 ± 235 and 651 ± 85 cpm, respectively.

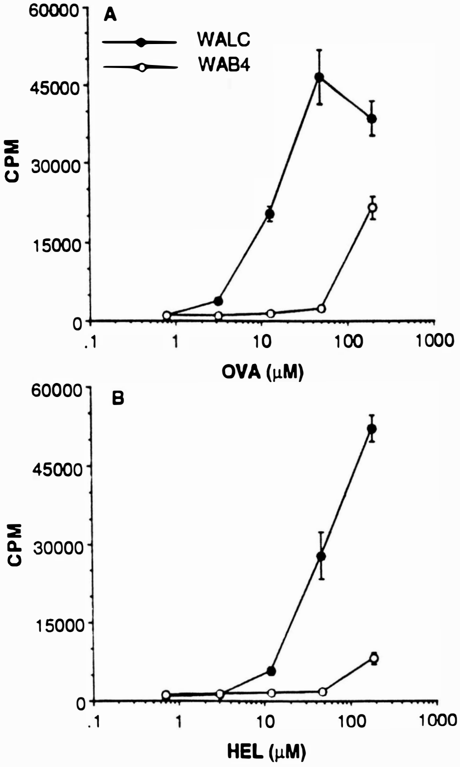
A
WALC
WAB4
CPM
60000
45000
30000
15000
0
.1
1
10
100
1000
OVA (μM)
B
CPM
60000
45000
30000
15000
0
.1
1
10
100
1000
HEL (μM)

and HEL, indicating that complementation occurred if each hamster chromosome was represented among the hybrid population of cells which was analyzed by karyotypic analysis.

4. Karyotypic analysis of the WALC hybrid population

Karyotypic analysis of the WALC hybrid population of cells was conducted in order to assess the relative representation of hamster and murine chromosomes among the hybrid population of cells. As shown in Table 1, there is preferential loss of murine chromosomes in the hybrid WALC line. In 11 karyotyped hybrid cells, a mean number of 28 out of 47 murine L cell-derived chromosomes were represented among the hybrid population of cells. This is in contrast to a mean number of 17 out of 20 hamster chromosomes found in the hybrid line. As shown in Table 2, all hamster chromosomes were present within the population of cells. The frequency of the individual hamster chromosomes varied from 2.4 to 0.7. This evidence suggests that restored processing in our hybrid cells is unrelated to the loss of any particular hamster chromosome.

5. A limited number of genes mediates the defect observed in WAB4 cells

To estimate the number of genes mediating the defect of WAB4, the hybrid population of cells was cloned via colony lift. Cloned populations of hybrid cells were expanded, and 28 clones were analyzed for MHC class II I-A^d expression and for antigen processing efficiency. As shown in Table 3, 28 cloned hybrid cells pulsed with a sub-optimal concentration of OVA (50μM) exhibited either 1 of three processing phenotypes: superior, intermediate, and poor. Those designated as superior (e.g. WALC.210) were more competent than the uncloned hybrid population of cells in eliciting a T cell response from 3DO-54.8 which was defined as responses greater than 28,000 cpm in the T cell assay. Superior clones elicited responses in a range from 29,000 cpm to 43,000 cpm. In one experiment, a total of 8 out of 17 clones were superior for processing. Intermediate clones (e.g. WALC.213) were so described

Table 1. Karyotypic analysis of the WALC hybrid population and parental WAB4 cells and L cells[a]

Cell type	**WAB4**	**L cells**	**WALC**
Mean # of mouse chromosomes	Absent	47	28
Mean number of hamster chromosomes	20	Absent	17

[a] Karyotypic analysis was conducted ny Genetic Research Inc. (Durham, NC). The number of cells karyotyped were 6, 10, and 11 for WAB4, L cells, and hybrid cells, respectively.

Table 2. Representation of hamster chromosomes among WALC hybrids[a]

Hamster chromosome number	**Mean number/cell**[b]
1	2.4
2	1.3
3	1.1
4	1.7
5	0.9
6	1.2
7	0.7
8	2.2
9	2.1
10	2.4
X	1.3

[a] See Table 1 legend.

[b] The mean number of individual chromosomes were averaged over all of the cells karyotyped.

Table 3. Antigen processing phenotypes among WALC clones[a]

Cell type	Superior	Intermediate	Poor
WAB4			4,000 cpm
WALC		16,400 cpm	
WALC.210	43,000 cpm		
WALC.213		16,405 cpm	
WALC.205			4,600 cpm

[a] The processing phenotypes for WALC clones were determined in the T cell activation assay described in the **MATERIALS AND METHODS # 3**. Those designated superior, intermediate, and poor elicited greater T cell responses than the uncloned hybrid line (≥29,000), comparable to the uncloned population (≥11,300), or as poorly as WAB4 cells (≥2,300), respectively, in the T cell assay.

because their ability to elicit responses from OVA-specific T cells was as good as the uncloned line of hybrids. As demonstrated in the T cell assay, the uncloned line WALC elicits responses at 16,400 cpm. Intermediate clones elicited responses in a range from 11,300 to 20,000. A total of 7 out of 17 were intermediate for processing OVA. Those designated as poor (WALC.205) processed OVA as poorly as WAB4 cells (4,000 cpm). These clones elicited responses in a range from 2,300 to 4,600 cpm in the T cell assay. A total of 2 out of 17 were designated as poor. The finding that all clones examined fell into 3 discrete categories argues that there are a limited number of genes mediating the defect or that the defect involves a gene dosage effect. Considering the finding that there is preferential retention of hamster chromosomes in the murine/hamster hybrids (Table 1), restoration of the antigen processing defect due to hamster chromosome loss would be expected to be less frequent than what was observed in these studies. However, in one experiment, the vast majority of clones were competent APC, suggesting the defect is not the result of hamster chromosome loss.

6. MHC class II expression by hybrid clones

Because T_h cell activation is dependant upon recognition of MHC class II molecules complexed with stimulatory peptide, we determined the impact of the level of class II expression among our hybrid clones. Though the expression of MHC class II molecules varied among different clones, staining for clones 205, 206, and 201 is identical as indicated by mode fluorescence intensity (Table 4). Interestingly, each of the latter three clones possessed the three distinct processing phenotypes described in section 5 of this chapter. As shown in **Figure 9**, a dot plot of processing efficiency vs. MHC class II expression was constructed to determine whether there existed a correlation with processing efficiency and MHC class II expression. Both processing efficiency and MHC class II expression were rated on a scale of 1 to 3. Those clones receiving

Table 4. Mode fluorescent intensity of MHC class II expression among WALC clones[a]

Cell type	**Mode Fluorescence**
WAB4	27
TA3	32
WALC	35
WALC.205	40
WALC.206	40
WALC.201	40

[a] Mode fluorescence intensity of MHC class II I-A^d expression among WALC clones was determined as described in the **MATERIALS AND METHODS # 7**.

Figure 9. Dot plot analysis of MHC class II (Ia) expression and processing efficiency among hybrid clones. Twenty-eight hybrid clones were scored on a scale of one to three for their expression of class II and ability to process OVA. A score of three was given to clones expressing higher levels of MHC class II molecules than the B cell lymphoma TA3, as indicated by mode fluorescence. Those scoring a two were equivalent to TA3 cells, and those scored as a one expressed lower levels than TA3 cells. A score of three for processing was given to clones capable of stimulating greater responses than the uncloned hybrid line in the Il-2 T cell assay (see Table 3 legend). Those scored a two and one were so designated if they elicited comparable or lower responses than the uncloned WALC line, respectively.

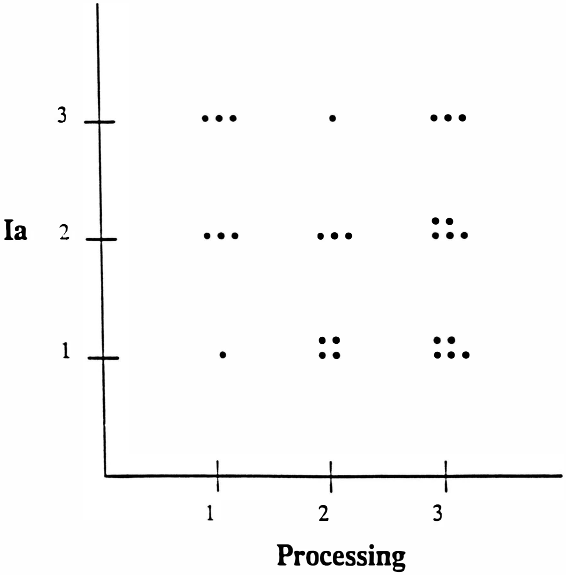
Ia
3
2
1
1
2
3
Processing

a score of 3, 2, or 1 for antigen processing were superior, intermediate,and poor, respectively for processing OVA as demonstrated in a T cell assay. Those clones receiving a 3, 2, or 1 for MHC class II expressed

higher, comparable, or lower mode fluorescence levels of I-A^d, respectively when compared to the effective B cell lymphoma APC, TA3. Constructing a dot plot summarizing the data for class II expression and processing efficiency of 28 clones reveals that the ability of WALC clones to process OVA is unrelated to Ia expression and is virtually random (**Figure 9**).

7. Surface expression of MHC class I molecules by hybrid clones

Because of the involvement of MHC-encoded proteins in antigen processing, we determined whether or not there was a correlation with the presence of surface expression of MHC class I H-2K^{k}D^k protein, which maps to murine chromosome 17, in our hybrid clones and processing proficiency. To that end, the level of expression of murine MHC class I molecules was assessed using flow cytometry and culture supernatants from the murine cell line 15-1-5P which recognize MHC class I H-2K^{k}D^k molecules. **Figure 10** is the staining of parental L cell fibroblasts for the 15-1-5P determinant. Because expression of murine chromosome 17-encoded MHC class I H-2K^{k}D^k molecules were being assessed in the hybrid clones, we used L cells which are the source of murine chromosome 17 in the hybrids as the standard for MHC class I expression.

A total of 18 clones were examined for MHC class I expression. **Figure 10** shows a representative histogram profile of WALC.204 clone demonstrating positive staining for MHC class I expression. Though WALC.204 clone expressed MHC class I molecules, it was poor for processing OVA. For the 18 clones examined, 22% of clones stained positively for the 15-1-5P epitope, but only 50% were superior for processing OVA suggesting that presence of MHC class I molecules, which

Figure 10. H-2K^{k}D^k class I expression among WALC clones. APC were washed, stained for MHC class I expression, and analyzed by flow cytometry as described in the **MATERIALS AND METHODS**. Fluorescence intensity of 10,000 cells was collected with logarithmic amplification. APC were incubated with saturating amounts of 15-1-5P and FITC-anti-mouse antibodIies (solid line) or FITC-anti-mouse antibodies alone (dashed line). A. DCEK Hi7 L cells. B. WAB4 cells. C. WALC.204 cells.

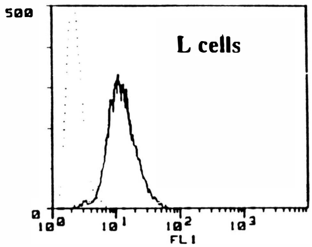
500
L cells
0
10^0
10^1
10^2
10^3
FL1

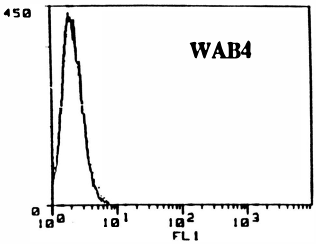
450
WAB4
0
10^0
10^1
10^2
10^3
FL1

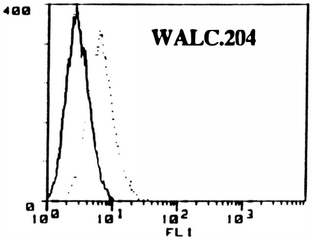
400
WALC.204
0
10^0
10^1
10^2
10^3
FL1

maps to chromosome 17, does not correlate with rescue of the processing defect of WAB4. If the presence of murine chromosome 17 correlated with rescue of the antigen processing defect of WAB4, clones superior, intermediate, and poor for processing would express high, intermediate, and low levels, respectively of MHC class I molecules.

8. **Invariant chain expression**

To define the Ag processing defect, we assessed the competency of WAB4 cells for each of the known steps of the MHC class II processing pathway. To that end, the hybrid WALC and parental L cells were examined for the intracellular expression of Ii chain by immunofluorescence staining of fixed cells. Although the L cell transfectants utilized in these experiments express mRNA for Ii chain (38), the protein was barely detectable by FACS (**Figure 11A**). Similarly, no significant staining was found for hybrid WALC cells with the mAb (**Figure 11B**). TA3 cells were used as a positive control and brightly stained for Ii chain (**Figure 11C**). The parental CHO cells were not included in these analyses, because the mAb In-1 is specific for murine Ii chain (80) and does not cross-react with the hamster protein. If hybrid cells express Ii chain, this would suggest correlation with the ability of the hybrids to process antigen. However, the expression of Ii chain did not correlate with the ability of the hybrid cells to process OVA and HEL and as a result the expression of Ii chain among hybrid clones was not determined.

9. **Normal levels of aspartic acid proteolytic activity**

Because the defect of WAB4 involves the generation of stimulatory peptide fragments from intact protein (**Figure 7**), we measured the levels of proteases, known to be important for Ag processing, in the WAB4 cells and compared to other competent APC. Other investigators have reported that acidic aspartyl proteases, such as cathepsin D, are crucial for the generation of stimulatory OVA peptides recognized by 3DO-54.8 cells (53-55). To examine the possibility that diminished proteolysis caused the

Figure 11. Low expression of the Ii chain cytoplasmic domain epitope In-1 by APC. The various APC were fixed, stained for Ii chain expression, and analyzed by flow cytometry as described in the materials and methods. Fluorescence intensity of 10,000 cells was collected with logarithmic amplification. APC incubated with saturating amounts of In-1 and FITC-MAR 18.5 (solid line) or FITC-MAR 18.5 alone (dashed line). A. DCEK Hi7 L cells. B. WALC hybrid cells. C. TA3 cells.

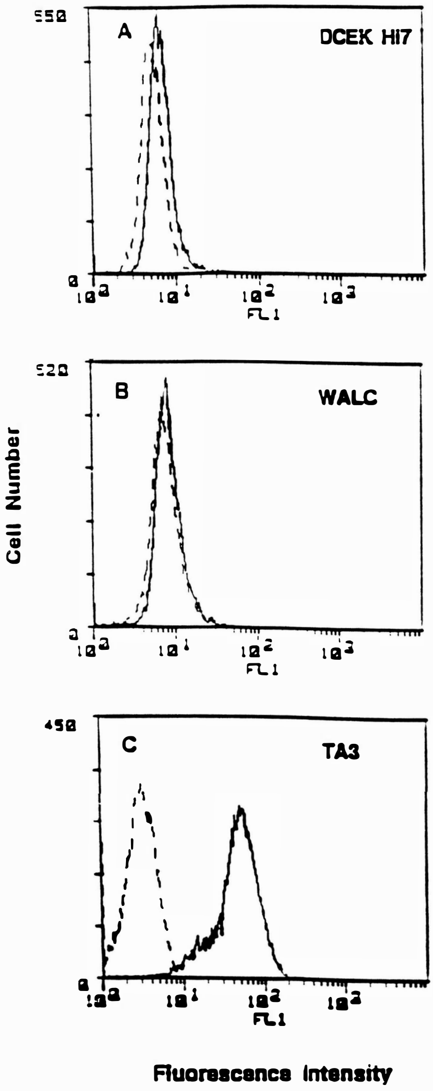
550
A
DCEK HI7
0
10^0
10^1
10^2
10^3
FL1
520
B
WALC
0
10^0
10^1
10^2
10^3
FL1
450
C
TA3
0
10^0
10^1
10^2
10^3
FL1
Cell Number
Fluorescence Intensity

Ag processing defect, we compared the level of aspartyl proteolytic activity in TA3 and WAB4 cells. Total cell lysates from WAB4 cells tended to contain more aspartic acid proteolytic activity than those from TA3 cells (2.56 ± 1.08 vs. 0.97 ± 0.72 units of activity per mg protein for WAB4 and TA3, respectively. The intracellular distribution of the proteolytic activity in WAB4 cells was investigated by separating organelles from disrupted cells by density centrifugation on a Percoll gradient. The relative distribution of the intracellular enzymatic activity for TA3 and WAB4 cells differed slightly. The maximal proteolytic activity in TA3 cells sedimented in fraction 13 (**Figure 12A**). By contrast, the highest level in WAB4 cells was located in the slightly less dense fraction 11 (**Figure 12B**). In addition, the profile of the protease activity was broader in the lysate from WAB4 cells than that from TA3 cells. However, for both TA3 and WAB4, those fractions containing peak levels of the lysosomal enzyme, β-galactosidase, possessed the greatest aspartyl proteolytic activity. Furthermore, the aspartyl proteolytic activity in all fractions from WAB4 cells was higher than that of the corresponding fractions from TA3 cells. Consequently, low aspartyl proteolytic activity in WAB4 cells cannot explain the poor ability of WAB4 cells to stimulate 3DO-54.8 cells with native OVA.

10. The effect of carbohydrate residues on processing of OVA by WAB4 cells

The possibility that the presence of carbohydrates may have interfered with the OVA processing by WAB4 cells was examined. N-linked high mannose residues on OVA were cleaved via endoglycosidase-H treatment. Glycosylated and unglycosylated forms of OVA were separated by Con A-Sepharose affinity chromatography, tested for degree of glycosylation by ELISA, and incorporated in T cell assays to measure potency. As shown in **Figure 13A**, for each form of OVA, TA3 readily induced comparable responses by the OVA-specific, I-A^d-restricted, T_h cell

Figure 12. WAB4 cells possess normal levels of aspartyl proteolytic activity. Lysates from 5 X 10^7 cells in 0.25 M sucrose/20 mM HEPES were prepared by N_2 cavitation, and postnuclear supernatants were fractionated on a 17.5 ml 23% Percoll gradient. One-ml fractions were collected and are numbered from the top of the gradient. Density bead markers were used to estimate the density profile (closed rectangles). Protein concentration was determined for each fraction via BCA assay. Enzymatic activities were determined for each fraction as described in the **MATERIALS AND METHODS**. Lysosomal β-galactosidase activity (open circles) are expressed in fluorescence units. Aspartyl proteolytic activity (closed circles) was measured in organelles disrupted by detergent. Values represent the mean total proteolytic activity per mg protein minus the mean non-aspartic acid proteolytic activity per mg protein from two experiments. *(A)* TA3 cells *(B)* WAB4 cells.

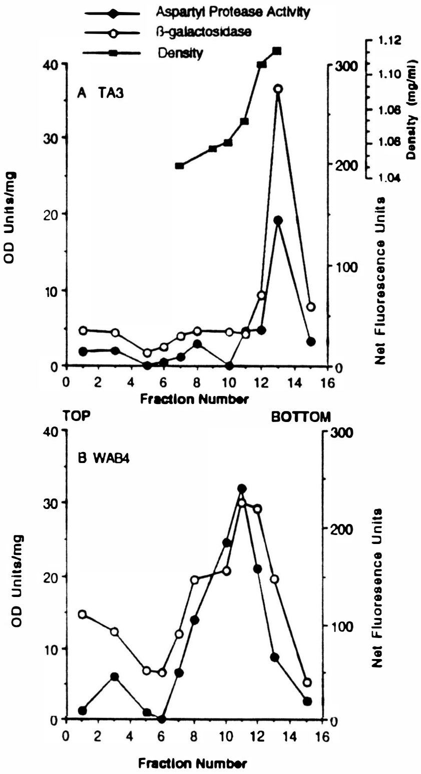
Aspartyl Protease Activity
ß-galactosidase
Density
A TA3
OD Units/mg
Net Fluorescence Units
Density (mg/ml)
1.12
1.10
1.08
1.06
1.04
0
10
20
30
40
0
100
200
300
0
2
4
6
8
10
12
14
16
Fraction Number
TOP
BOTTOM
B WAB4
OD Units/mg
Net Fluoresence Units
0
10
20
30
40
0
100
200
300
0
2
4
6
8
10
12
14
16
Fraction Number

Figure 13. Endoglycosidase-H treatment of OVA. OVA at 45/mg/ml was suspended in 0.05 M citrate buffer with or without 450 milliunits of endoglycosidase-H. Enzyme treatment was allowed to proceed for 20 h at 37°C. Glycosylated and unglycosylated OVA was separated via Con A-Sepharose affinity chromatography. The extent of glycosylation of all OVA preparations was determined by ELISA. Preparations of glycosylated (circles) and unglycosylated OVA (squares) were obtained with (filled symbol;Endo-H) or without (empty symbol;mock) enzyme treatment and were incorporated in a T cell activation assay along with untreated native OVA (triangle) using TA3 (A) or WAB4 (B) as the source of APC.

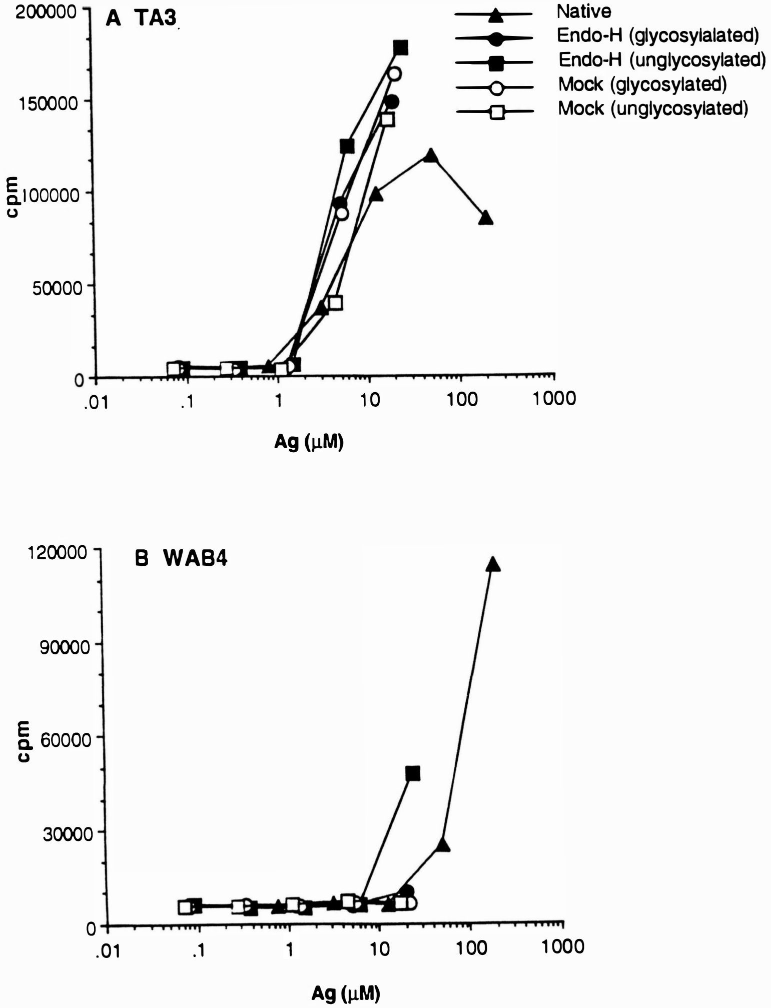
A TA3
200000
150000
100000
50000
0
cpm
.01
.1
1
10
100
1000
Ag (μM)
Native
Endo-H (glycosylalated)
Endo-H (unglycosylated)
Mock (glycosylated)
Mock (unglycosylated)
B WAB4
120000
90000
60000
30000
0
cpm
.01
.1
1
10
100
1000
Ag (μM)

hybridoma 3DO-54.8, suggesting that the degree of glycosylation had no bearing on the ability of TA3 to generate stimulatory peptides of OVA. However, when WAB4 (**Figure 13B**) were the source of APC, the removal of carbohydrate via endo-H treatment increased antigenic potency compared to the native form of OVA (**Figure 13B**). The increase in antigenic potency following endo-H treatment has become difficult to interpret with the finding that OVA preparations passed over the Con A-sepharose column stimulated T cells specific for pigeon cytochrome c (data not shown), indicative of Con A contamination which is a T cell mitogen.

11. **Reduction of OVA and HEL restores normal processing by WAB4 cells**

The one shared biochemical characteristic among pork insulin, OVA, and HEL which were not processed well by WAB4 cells was the presence of disulfide bonds (Table 5). To determine whether the presence of disulfide bonds correlated with the ability of WAB4 to process disulfide bond containing antigens, reduced/alkylated OVA (CM-OVA), reduced OVA (D-OVA), and reduced/alkylated HEL (CM-HEL) were analyzed for their antigenic potency. Insulin was excluded, because derivatization of Cys residues causes the loss of antigenicity (66). Analysis of the helical character by circular dichroism Helical character for each protein was determined by comparing millidegree values at 220 nm for each protein which was 6.03, -38.27, -8.36, -3.64, -1.40 for CM-HEL, N-HEL, N-OVA, CM-OVA, and D-OVA, respectively revealed extensive loss of secondary conformation of D-OVA, CM-OVA, (Figure 14) and CM-HEL (Figure 15) compared with native Ag. Paraformaldehyde-fixed APC presented OVA and HEL peptides, but not D-OVA, CM-OVA, nor CM-HEL (data not shown), indicating that the reduced preparations of OVA and HEL required processing.

As shown in **Figure 16A** and **B**, the T cells responded to both D-OVA and CM-OVA when the positive control TA3 cells were the source of the APC, as expected. A dramatic improvement in the ability of WAB4 cells

Table 5. Correlation of presence of disulfide bonds in the Ag processing defect of WAB4 cells.

Antigen	**Disulfide bond(s)**	**Processed**[a]
Pigeon cytochrome *c*	0	Yes
Lambda repressor	0	Yes
Staphylococcal nuclease	0	Yes
Pork insulin	**2**	**No**
Hen egg lysozyme	**4**	**No**
Ovalbumin	**1**	**No**

[a] Ability to process was determined in a T cell activation assay as described in the **MATERIALS AND METHODS # 3** using WAB4 cells as the source of APC.

Figure 14. Extensive loss of secondary structure of OVA after reduction. Circular dichroism was performed on native OVA, CM-OVA, and D-OVA at 200μg/ml in H_2O under N_2 atmosphere. The mdeg at various wavelengths in nm is illustrated. Helical character of the protein was determined by mdeg at 220nm.

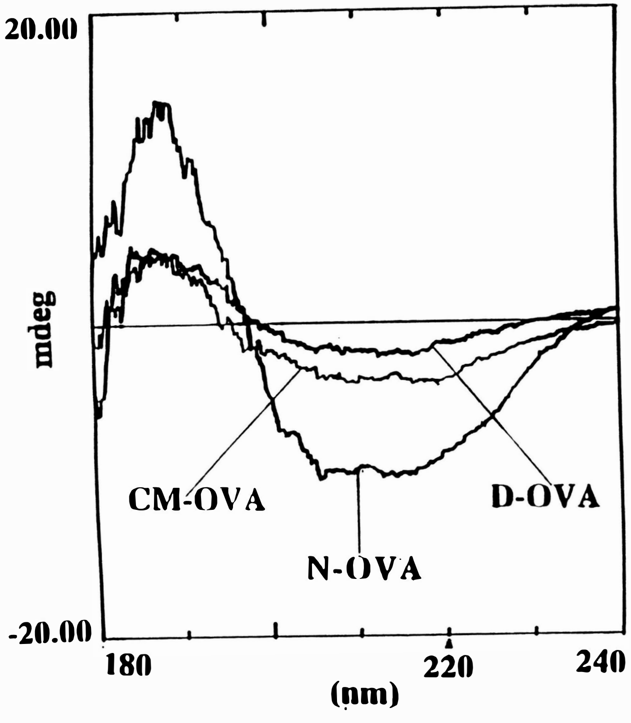
20.00
-20.00
mdeg
CM-OVA
D-OVA
N-OVA
180
220
240
(nm)

Figure 15. Circular dichroism analysis of HEL. Helical character of native HEL and CM-HEL was determined (**Figure 13 legend**) as described in the **MATERIALS AND METHODS.** Helical character of the protein was determined by mdeg at 220nm.

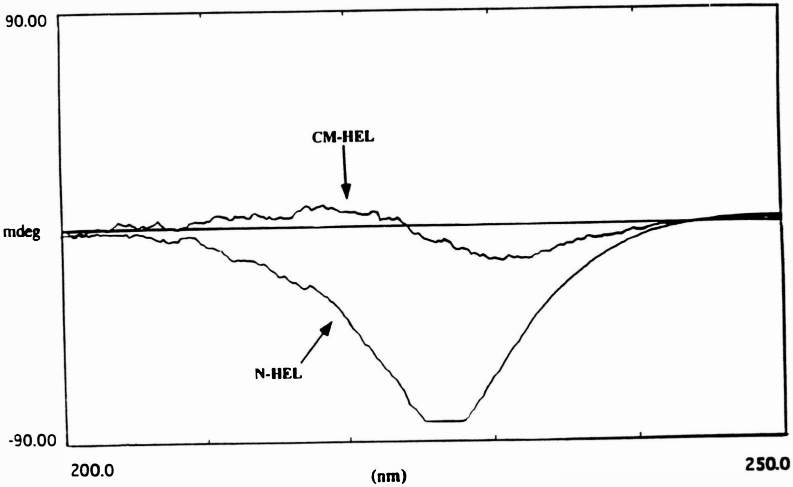
90.00
mdeg
-90.00
200.0
(nm)
250.0
CM-HEL
N-HEL

Figure 16. Restoration of processing by reduction of OVA and HEL. IL-2 response of T cells with TA3 (closed circles) and WAB4 cells (open circles) as the APC (**see Figure 1 legend**). *(A)* Response of 3D0-54.8 to D-OVA. *(B)* Response of 3D0-54.8 to CM-OVA. *(A)* and *(B)* are from the same experiment which is representative of four. The medium controls for WAB4 and TA3 cells were 3,411 ± 472 and 1,534 ± 58 cpm, respectively. *(C)* Stimulation of 9.30.B2 with CM-HEL. The medium controls for WAB4 and TA3 cells were 1,045 ± 175 and 1,119 ± 342 cpm, respectively. The experiment is representative of three.

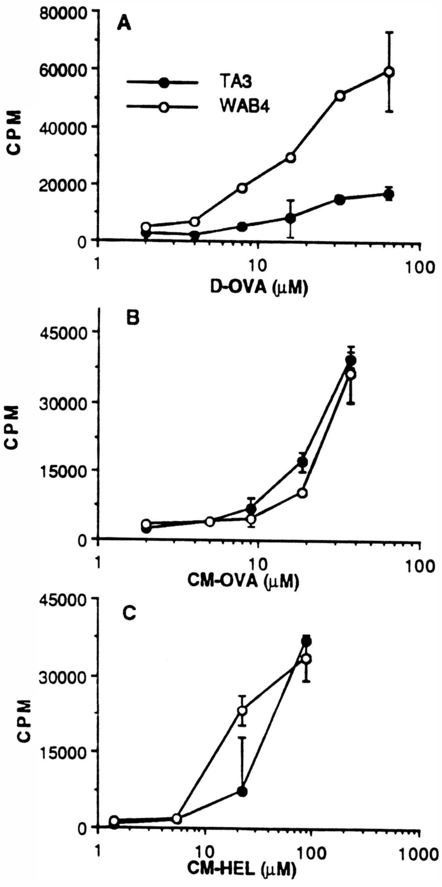
A
TA3
WAB4
CPM
80000
60000
40000
20000
0
1
10
100
D-OVA (μM)
B
CPM
45000
30000
15000
0
1
10
100
CM-OVA (μM)
C
CPM
45000
30000
15000
0
1
10
100
1000
CM-HEL (μM)

to stimulate the T cells was observed with the denatured forms of OVA. With WAB4 cells as the APC, T cell responses were induced by 8 μM D-OVA and 19 μM CM-OVA, whereas native OVA was non-stimulatory at these concentrations (see **Fig. 6** **C**). Interestingly, D-OVA, which contained a reduced disulfide bond, was processed more efficiently by WAB4 than the CM-OVA preparation, which is reduced and alkylated, suggesting that disulfide bond reduction alone may be the deficient step in WAB4-mediated Ag processing. Therefore, extensive derivatization of the 6 cysteines in OVA with iodoacetic acid may inhibit the efficiency of protease-mediated generation of stimulatory peptides of OVA by WAB4 cells. The presence of 50 μM 2-mercaptoethanol in the medium did not affect the potency of any forms of OVA (data not shown). Analogous results were also observed for CM-HEL (**Fig. 16** **C**). In contrast to native HEL (see **Fig. 6** **B**), WAB4 cells readily induced a T cell response to CM-HEL to a level that was comparable to that of TA3 cells. These findings were obtained with multiple preparations of reduced Ag and were not unique to one preparation, indicating that the processing defect of WAB4 cells may be related to a poor ability to unfold Ag containing disulfide bonds.

12. Decreased cleavage of disulfide bonds

Because normal Ag processing was restored to WAB4 cells by reducing Ag containing disulfide bonds, it seemed likely that WAB4 possessed a defect in disulfide bond reduction. To address directly this potential defect, the ability of WAB4 cells was compared with that of the cell hybrid WALC to cleave endocytosed disulfide bonds. Cells, whose surface membranes were labeled with ^{125}I-tyn-SS-PDL at 0°C, were allowed to internalize the iodinated conjugate at 37°C up to 2 h. At the end of the incubation, additional reductive cleavage was blocked with the permeant sulfhydryl inhibitor, N-ethylmaleimide. The reduction of ^{125}I-tyn-SS-PDL, which is resistant to proteolysis (84), was determined by the release of TCA-soluble 3-thiopropionyl-^{125}I-tyramine. As shown in **Figure 17**, the

Figure 17. Diminished reduction of disulfide bonds. WAB4 cells (open circles) or WALC hybrid cells (closed circles) were incubated with ^{125}I-tyn-SS-PDL at 37°C for up to 2 h as described in the **MATERIALS AND METHODS**. The extent of reductive cleavage of the conjugate was measured as the release of TCA-soluble radioactivity. Values are the mean percentage of TCA-soluble radioactivity ± SD from two experiments with duplicate cultures. Statistical analysis was performed by ANOVA. WAB4 vs. WALC at 90 min and 120 min: $p < 0.005$.

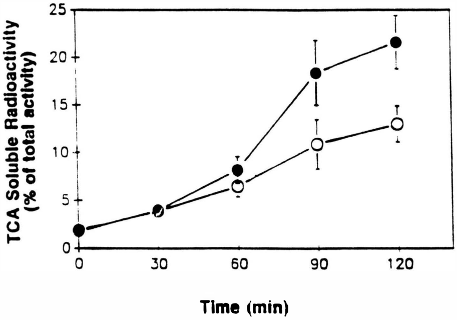
TCA Soluble Radioactivity
(% of total activity)
25
20
15
10
5
0
0
30
60
90
120
Time (min)

percentage of TCA-soluble radioactivity increased as a function of time. Initially, the level of radioactivity generated by the two cells was similar. However, WAB4 cells had deficient reductive capacity compared to the cell hybrid WALC at the later time points. The most rapid reduction of the conjugate occurred between 60 and 90 min, and WAB4 cells displayed the most pronounced defect in reduction during that same time interval. By the end of the time course, the degree of reduction of the conjugate by WAB4 cells was approximately half that by the cell hybrid.

13. Intracellular levels of cysteine and glutathione

It has been reported that the lysosomes may serve as the intracellular site of disulfide bond cleavage (67, 87). The intent was to dissect the mechanism by which lysosomes maintain an environment suitable for reductive cleavage (**see Figure 5**) and analyze the proficiency of this environment in the defective WAB4 cells.

Based on these observations, we measured intracellular levels of GSH and cysteine in cell lysates. As shown in table 6, intracellular levels of GSH in defective WAB4 cells were lower than GSH levels in lysates from other cells known to be proficient APC. WAB4 cells had 50-73% of the quantity of GSH on a per mg of protein basis compared to the other cells. The hybrid line 125 was generated during the same fusion as the hybrid WALC. The distinction between 125 and WALC results from duration respective lines were maintained in culture. In addition, intracellular levels of cysteine were measured in a series of lysates generated from a variety of competent APC. As shown in Table 6, WAB4 did not seem to possess significantly lower nmol/mg lysate protein of cysteine when compared to the hybrid 125. In addition, WAB4 seems to possess comparable levels of nmol/mg lysate protein of cysteine compared to the macrophage line clone 63 and the B cell lymphoma TA3, suggesting that the defect of WAB4 may not involve deficient intracellular levels of cysteine.

Table 6. Intracellular levels of GSH and cysteine[a]

Cell type	Cysteine	GSH
WAB4	2.26 ± 0.44	0.54 ± 0.24
125	3.76 ± 2.72	1.0 ± 0.12
TA3	1.74	0.93
Clone 63	2.15	0.74

[a] Intracellular levels of GSH and cysteine in cell lysates were measured according to the methods of Tietze (86) and Gaithonde (85), respectively. Values are nmol/mg protein ± SD.

14. Cysteine transporter activity

In order to support lysosomal reductive cleavage, cysteine must be transported from the cytoplasm into the lysosome via a lysosomal-specific cysteine transporter. In order to assess the integrity of this transporter in defective WAB4 cells, the level and distribution of transporter activity was measured in WAB4 cells and the hybrid 125 cells. These cells were labelled with [^{35}S]cystine for 15 minutes and the distribution of radioactivity in granular pellets was examined. In three separate experiments there was no observable difference in the level of transporter activity in granular pellets from WAB4 and WALC hybrid cells when the data were normalized for differences in lysosomal and β-galactosidase activity (data not shown). In some experiments, the granular pellets of WAB4 and the hybrid 125 were fractionated to determine the distribution of transporter activity among intracellular organelles. As shown in **Figure 18**, the major distribution of activity resolved into two peaks for both WAB4 and WALC hybrid cells. As determined by density marker beads and β-galactosidase activity (data not shown), these peaks represented fractions enriched for endosomes (fractions 8-11) and lysosomes (fractions 22-24). Though both cell types possessed transporter activity in endosomal and lysosomal fractions, the hybrid cells had greater activity in the lysosomal fractions compared to the endosomal fractions. The distribution of activity in endosomal and lysosomal fractions was more equitable in the WAB4 cells which may have an impact on the overall levels of cysteine found within the lysosomes of WAB4 cells.

15. Inhibition of Glutathione synthesis in WALC hybrid cells.

In order to assess directly the effect of intracellular levels of GSH on antigen processing, the hybrid WALC cells, known to process competently Ag containing disulfide bonds (**see Figure 7**), were incubated with the τ-glutamyl synthetase inhibitor BSO. Hybrid cells were pre-

Figure 18. Cysteine-specific transporter activity in WAB4 and 125 hybrid cells. The activity of the cysteine-specific transporter was measured as described by Pisoni et al (87). Cells were labeled with [^{35}S]-cystine for 15 minutes at 37°C. Lysates were prepared by N_2 cavitation, and granular pellets were generated centrifugation as described in the **MATERIALS AND METHODS**. The granular pellets from WAB4 (Square) and hybrid 125 (diamond) cells were fractionated by Percoll density gradients. The level of radioactivity in cpm was measured in one-ml fractions collected from the top of he gradient.

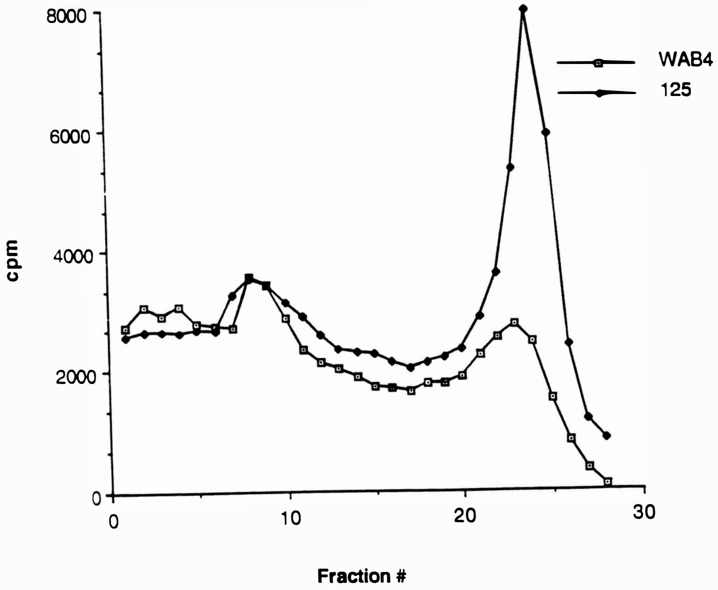
8000
6000
4000
2000
0
cpm
0
10
20
30
Fraction #
WAB4
125

treated up to 24 h with BSO, pulsed with a sub-optimal concentration of HEL for 5 h, and tested for Ag processing competency in a T cell assay. Concomitant with Ag pulse, intracellular levels of GSH and cysteine were determined in cell lysates generated from hybrid cells. Treatment of hybrid cells in two separate experiments resulted in 90% loss of intracellular levels of GSH compared to mock-treated control cells. Cysteine levels of cysteine remained unaffected by BSO treatment (data not shown). As shown in Table 7, treatment of the hybrid cells with BSO in experiment 1 significantly affected the capacity of the hybrid cells to process HEL compared with untreated controls, suggesting that BSO treatment of WALC hybrid cells diminishes hybrid-mediated processing of HEL suggesting that intracellular levels of GSH may be important for antigen processing.

16. N-acetyl treatment of WAB4 cells

If intracellular levels of GSH correlate with the ability of APC to process Ag containing disulfide bonds, augmentation of GSH levels in WAB4 cells should improve WAB4-mediated processing of antigens containing disulfide bonds. To that end, WAB4 was treated with N-acetyl cysteine known to increase intracellular levels of GSH in lymphocytes (89). The rate-limiting step in the biosynthesis of GSH is the generation of τ-glutamyl cysteine from its constituent amino acids cysteine and glutamine via the action of τ-glutamyl synthetase. N-acetyl cysteine prevents diminished production of GSH by providing cysteine, which could otherwise be limiting, to the biosynthetic pathway for GSH. WAB4 cells were treated with N-acetyl cysteine for 9 h. The medium was removed and replenished with medium containing N-acetyl cysteine. Incubation was allowed to proceed for 12 h. The treatment protocol employed was reported to cause a 2-to 3-fold increase in GSH levels (89). WAB4 cells were pulsed with suboptimal concentrations of 50 μM HEL for 5 h and then tested for Ag processing proficiency in a T cell activation assay. Concomitant with

Table 7. BSO treatment of WALC hybrid cells[a].

Exp #	**Cell**	**T cell assay (cpm ± SD)**
1	(BSO) WALC	61,116 ± 2,493
1	WALC	73,894 ± 1,986
2	(BSO) WALC	67,163 ± 4,545
2	WALC	74,836 ± 1,474

[a]Hybrid cells were treated with BSO for 24 h. The cells were pulsed with suboptimal concentration of HEL for 5 h and tested for processing efficiency in a T cell activation assay (**see MATERIALS AND METHODS**). Concomitant with the pulse, intracellular levels of GSH and cysteine were measured as described in the **MATERIALS AND METHODS**. Statistical analysis was performed by unpaired two-tail Student's *t*-test. BSO vs. untreated: $p < 0.001$ and $p < 0.05$ for experiments 1 and 2, respectively.

Ag pulse, intracellular levels of GSH were measured. Although N-acetyl cysteine should have elevated GSH levels (89), we were unable to detect any increase in intracellular levels of GSH by our assay (data not shown). However, treatment of WAB4 with this reagent resulted in significant augmentation of T cell responses (Table 8). One possible explanation for the lack of augmentation of GSH in treated cells may be the sensitivity of our assay. An alternative method that has greater sensitivity employs high-performance liquid chromatography (89), which was unavailable for these studies.

Table 8. N-acetyl treatment of WAB4 cells[a].

Exp #	**Cell**	**T cell assay (cpm ± SD)**
1	WAB4(NAC)	26,659 ± 1,806
1	WAB4	19,082 ± 2,513
2	WAB4 (NAC)	39,643 ± 2,668
2	WAB4	25,423 ± 1,026

[a]N-acetyl cysteine treatment of WAB4 cells was conducted as described in the **MATERIALS AND METHODS**. WAB4 cells were pulsed with 50 μM of HEL and measured for their ability to elicit a T cell response as described in the **MATERIALS AND METHODS**. Statistical analysis was performed by unpaired Student's two-tail *t*-test NAC treated vs. untreated $p < 0.01$ and $p < 0.001$ for experiments 1 and 2,respectively.

DISCUSSION

We investigated the ability of a CHO transfectant to stimulate a panel of T_{1h} cells specific for a variety of Ag. These APC cells were fully capable of inducing T cell responses to native pigeon cytochrome c, Staphylococcal nuclease (48), and λ-repressor as shown in this dissertation. By contrast, the CHO cells were very poor in activating T cells specific for intact OVA, HEL, and pork insulin, whereas peptide presentation by these APC was normal.

Genetic complementation analysis demonstrated that a hybrid, generated by the fusion of CHO cells and L cell fibroblasts, processed native OVA and HEL indicating a recessive defect. Any possible suppressive effects that the CHO cells may have had on a T cell response are unlikely, because suppression should be a dominant characteristic. Karyotypic analysis revealed that each hamster chromosome was represented among the hybrid population of cells. This provided evidence suggesting that processing restoration observed in the hybrid cells was a result of murine chromosomal gain and not hamster chromosomal loss. Characterization of processing ability among hybrid clones demonstrated the greater percentage of hybrid cells were superior in processing a suboptimal concentration of OVA. Because there is preferential loss of murine chromosomes in a mouse/hamster hybrid, the finding that the majority of clones are superior for processing lends additional support to the argument of a recessive defect complemented by murine chromosomes. Surface expression of MHC class I molecules did not correlate with the hybrid clones ability to process Ag which suggests genes present on murine chromosome 17 are not responsible for complementation of the WAB4 defect.

The effect of carbohydrate moieties on Ag processing remains uncharacterized. Because OVA is glycoprotein (90, 91), we investigated whether removal of carbohydrate moieties from OVA would improve its processing by the defective cells. One possible candidate for the recessive defect is that WAB4 could lack deglycosylating enzymes necessary for efficient processing of OVA. Absence of this enzyme would be consistent with the recessive nature of the WAB4 defect. Our results utilizing Endo-H-treated unglycosylated and glycosylated forms of OVA demonstrate that removal of these moieties from OVA results in a 10-fold improvement in the ability of WAB4 to elicit a response from T cells when OVA is stripped of carbohydrate groups. In contrast, mock-treated OVA lacking intact carbohydrate moieties, does not improve WAB4-mediated processing. The only known carbohydrate feature shared by Endo-H- and mock-treated unglycosylated OVA samples is the lack of mannosyl residues recognizable by the Con A column. In addition, the conformation of mock- or Endo-H-treated proteins was unchanged compared to that of intact untreated OVA as shown by circular dichroism analysis and no protein fragmentation was detected by SDS-PAGE (data not shown). Thus, one possible explanation for this apparent contradiction is other distinctions in carbohydrate structure remain undetected. On the other hand, the presence or absence of these carbohydrate groups did not seem to affect TA3-mediated activation of OVA-specific T cells. This finding may be explained by the fact that TA3 are extremely competent APC. Therefore, by merely bypassing a step in processing for which TA3 cells are already completely functional did not enhance TA3-mediated T cell activation. Because the affinity column was made up of Con A, a T cell mitogen, it was important to determine whether or not all affinity chromatography obtained OVA preparations were contaminated with Con A. These experiments showed that APC were able to elicit a response from the pigeon cytochrome c-specific T cell hybridoma 2B4 using affinity-purified OVA as the source of Ag. These results suggest that Con A was present in the column-derived OVA preparations and as a result have made complicated interpretation of these results.

Aspartyl cathepsins D and E have been implicated as the enzymes mediating the processing of native OVA to stimulatory peptides recognized by the T cells in our study (53-55). However, the proteases required for the processing of the other Ag have not been conclusively identified. Because OVA was among the three Ag improperly processed by CHO cells, aspartyl proteolytic activity in these cells was analyzed. Our experiments indicates that total cell lysates from CHO cells possessed slightly greater amounts of aspartyl proteolytic activity than that from a B lymphoma cell, an APC efficient at processing OVA. Furthermore, analysis of the enzymatic content of separated organelles in gradient fractions revealed that the CHO cells contained greater proteolytic activity in all their fractions than those from the B cells. Thus, diminished aspartyl proteolytic activity was not the mechanistic basis for the OVA processing defect expressed by the CHO cells. The recessive nature of this defect also rules out the possibility that impaired Ag processing results from elevated levels of proteases which would be expected to be a dominant trait if it led to destruction of the antigenic determinant.

Recent investigations have emphasized the importance of Ii chain in processing exogenous Ag (40, 92). Although CHO cells do not express any detectable levels of Ii chain mRNA (K.L. McCoy, unpublished observation), the possibility that the lack of Ii chain is responsible for the processing defect of these cells is questionable. L cells, the fusion partner, express mRNA for Ii chain mRNA (38). A cytoplasmic stain for Ii chain revealed low and no expression of this protein inside the L cells and the cell hybrid, respectively, in marked contrast to a B lymphoma cell. Yet, the cell hybrid was capable of processing both OVA and HEL, whereas the parental CHO cells were extremely poor in this function. Because the hybrid line of cells expressed low levels of Ii chain protein, clones of the hybrid line were not examined for Ii chain expression. The possible contribution of the absence of Ii chain to the impaired Ag processing exhibited by CHO cells requires additional studies.

Our results showing that Ag lacking disulfides were processed normally while those containing disulfides were not processed well by the CHO cells suggest a possible defect in disulfide reduction, and such a defect would be a recessive trait. In agreement with this possibility, normal processing of OVA and HEL by the CHO cells was restored merely by modifying the Ag. Because the CHO cells readily processed denatured and reduced forms of OVA and HEL, the CHO cells must be capable of presenting the correct peptide fragments and providing the necessary co-stimulatory signals to the T cells. In addition, the normal presentation of the reduced forms of HEL and OVA by the CHO cells suggests that diminished Ag internalization is an unlikely explanation for the processing defect, because carboxymethylated Ag should enter the cells by fluid-phase endocytosis similar to native Ag. Furthermore the enhanced processing efficiency of D-OVA and CM-OVA by the CHO cells indicates that reduction of disulfides is an important step in the processing of OVA by APC.

The decreased capacity of the CHO cells to reduce the disulfide linked ^{125}I-tyn-SS-PDL probe compared with the hybrid WALC strongly supports the hypothesis that decreased disulfide reduction of Ag causes the defective Ag processing. Because the conjugate consists of only D-amino acid residues, it is not susceptible to proteolysis and is stable at acid pH (84). Therefore, the generation of TCA-soluble fragments reflects cellular capacity to cleave only disulfide bonds. Because each lysyl residue carries a positive charge, the conjugate avidly binds to the cell membrane and is efficiently internalized by absorptive endocytosis. Previously it has been shown that in the first 15 to 30 min, following attachment to the surface membrane, disulfide reduction is blocked by impermeant thiol reagents, such as Ellman's reagent or p-chloromercurobenzoylsulfonate, suggesting that during this time interval reduction occurs only at the cell surface (84). Because the degree of cleavage of the conjugate is the same for both cell types in the first 30 min, the reductive capacity at their surface membranes must be equivalent. At later times, however, reductive cleavage is not inhibited by these thiol reagents, reflecting disulfide reduction in endocytic vesicles (84). Between 60 min and 2 h, the CHO cells showed significantly diminished cleavage of ^{125}I-tyn-SS-PDL, strongly indicating that these CHO cells have decreased vesicular capacity for intracellular disulfide reduction. Therefore, genetic complementation restores normal function. Such impaired processing of Ag with disulfide bonds resulting from diminished reductive capabilities is apparently the first example of an APC possessing such a defect.

The exact location and mechanism by which disulfide bonds in endocytosed macromolecules are reduced is presently unknown. Reduction of disulfide bonds of endocytosed protein conjugates has been shown to occur within lysosomes (67), although in some cases disulfide bonds remain intact during the transport of disulfide-linked protein conjugates (93). The acidic pH of lysosomes is unfavorable for disulfide reduction, although an acidic pH can prevent the oxidation of free sulfhydryl residues (94). The lysosomal membrane does, however, contain a transporter that translocates cytosolic cysteine into that organelle (87) where cysteine may serve as a reducing agent and may also influence the enzymatic activity of thiol proteases, such as cathepsin B, presumably by keeping the active site in a reduced state (94).

The efficiency of lysosomal-mediated reduction of disulfide bonds is predicated on maintaining sufficient levels of cysteine within the lysosomes. We examined the efficiency of key steps which are necessary for lysosomal reductive cleavage in the defective WAB4 cells. Cytosolic cystine is reduced to cysteine by GSH. Compared to lysates from a variety of different cell types, WAB4 had deficient intracellular nmol/mg levels of GSH. However, lysates from WAB4 cells possessed comparable levels of intracellular cysteine as compared to lysates from other cell types. This may be explained by the fact that there are other potential sources responsible for intracellular levels of intracellular cysteine. One of which is the GSH-mediated reduction of cystine to cysteine; the other sources are the extracellular supply of cysteine taken up at the cell's surface and de novo synthesis of the non-essential amino acid. Though GSH-mediated generation of cysteine may be affected in the WAB4 cells, it remains undetected because of the cysteine taken up at the surface of the cells or because of its ability to synthesize cysteine. It is also important to consider that despite the finding that total levels of cysteine are comparable to other cell types, it remains unknown what the lysosomal content of cysteine is in the WAB4 cells compared to other APC.

Using the τ-glutamyl synthetase inhibitor BSO, we successfully decreased the intracellular levels of GSH in the hybrid cells up to 90% of mock-treated hybrid cells. Similar to what we found in the defective WAB4 cells, diminished levels of GSH after to BSO treatment failed to affect intracellular levels of cysteine. Again, other sources,besides GSH reduction, may maintain intracellular levels of cysteine. However, as shown with the defective WAB4 cells, diminished levels of GSH correlate with an inability to process effectively Ag containing disulfide bonds. In our assay, the BSO-treated hybrid cells which displayed a 90% loss in intracellular levels of GSH, were no longer as effective at processing HEL compared to mock-treated control hybrid cells as demonstrated in the T cell activation assay.

The reciprocal experiment corroborated findings observed with the hybrid cells. If GSH levels were contributed to the defect observed in the WAB4 cells, increasing GSH levels in the WAB4 cells should enhance WAB4-mediated processing of Ag containing disulfide bonds. Though N-acetyl cysteine has been shown to increase by nearly two-fold (89) intracellular levels of GSH, we were unsuccessful in elevating intracellular levels of GSH in the WAB4 cells as determined by our GSH assay. This may be explained in part by our method of measuring GSH levels. The most sensitive method for measuring intracellular levels of GSH uses high performance liquid chromatography (89). Subtle, yet significant, changes in GSH levels may remain undetected by the Tietze method used by this laboratory (W.E. Samlowski., personal communication). Despite the fact that we were unable to detect changes in intracellular levels of GSH using N-acetyl cysteine, we did enhance WAB4-mediated processing of HEL. Though preliminary, these findings may suggest that intracellular levels of GSH affect the efficiency of antigen processing and that maintenance of GSH levels may be mechanism for the defect in the WAB4 cells. Additional studies will involve increasing the sensitivity for GSH detection and measuring GSH and cysteine levels in cell lysates and the lysosomes in medium devoid of these thiols.

Cysteine transporter activity at 15-min time point in granular pellets from defective WAB4 cells was comparable to that observed in granular pellets from hybrid cells suggesting that cysteine in the cytoplasm of WAB4 cells should be entering the lysosomes. A more exhaustive study involving time kinetics of transporter activity in WAB4 cells may prove to be more revealing. Does the activity in the WAB4 cells compare over time to the activity over time in the hybrid cells? Initial studies analyzing the distribution of radioactivity in subcellular fractions suggests that peak cysteine pump activity is found within fractions enriched for endosomes and lysosomes. The relative distribution of this activity among WAB4 cells and hybrid cells seems to vary however. The hybrid cells may have greater cysteine transporter activity in fractions enriched for lysosomes as compared to the endosomes. If cysteine is indeed necessary for intracellular disulfide cleavage, these data could suggest that endosomes and lysosomes may serve to reduce proteins containing disulfide bonds. Furthermore, if the lysosomes are the site for intracellular reductive cleavage, the fact that WAB4 may have lower cysteine transporter activity in lysosomal fractions may partly explain why the WAB4 cells are deficient in processing Ag with disulfide bonds.

Our findings are consistent with a model whereby disulfide reduction occurs at an early step in Ag processing. Previous evidence supports the viewpoint that protein unfolding and disulfide bond reduction are important events during Ag processing via the endocytic pathway (66-68). For example, reduction of disulfide bonds in insulin exposes two cysteine residues that are also within the antigenic determinant (66, 95). Other Ag, such as OVA, lack cysteine within the antigenic peptide, and maintain the need to be further processed by APC after denaturation and reduction, regardless of alkylation (96, 97). Reduction of BSA renders it more susceptible to proteolytic cleavage and shifts the pH optimum of cathepsin D to a higher pH (69). Similar findings were reported for HEL and RNase A (67). In some cases, denaturation alone circumvents the requirement for Ag processing. For example, S-methyl-myoglobin (98), disulfide-reduced apamin (99), and CM-HEL (100) can be presented by fixed APC to some T cell clones. In addition, reduction of disulfide bonds leads to the binding of some native Ag to fixed APC under acidic conditions (72). The exact consequence of disulfide cleavage varies depending on the Ag.

The impaired processing of Ag with disulfide bonds by the CHO cells correlated with diminished intracellular reductive capacity and may be associated with decreased intracellular levels of GSH and/or a change in the subcellular distribution of the cysteine transporter. Both the reductive capacity and the levels of GSH were enhanced in the cell hybrid. In addition, the relative distribution of cysteine transporter activity was different in the hybrid cells; peak levels of transporter activity were associated with the lysosomal fractions. All of these changes in the hybrid cells were concomitant with the restoration of normal Ag processing. When hybrids were treated with the reagent BSO, loss of efficient Ag processing was associated with a dramatic decrease in intracellular levels of GSH. The hybrids were; however, able to elicit sufficient responses despite a 90% drop in GSH. This may be explained in part by the fact that intracellular levels of cysteine in the hybrid cells were unaffected by BSO treatment. This may suggest that both cysteine and GSH play a role in the processing of Ag with disulfide bonds. The suggested problem of WAB4 having the capacity to maintain intracellular levels of GSH along with a possible inability to maintain peak levels of cysteine transporter activity at the lysosomal membrane are all consistent with a genetic defect involving a limited number of genes.

Because the defective WAB4 cells process Ag lacking disulfide bonds, either denaturation of these Ag is not as critical for their processing or occurs by a different mechanism, such as the acidic vesicular environment, that is present in these cells. The molecular structure of the Ag itself may thus dictate the level of stringency of the processing requirement. Therefore, further study of the CHO cells may reveal the mechanisms by which Ag are unfolded within the endocytic compartments during Ag processing.

LITERATURE CITED

LITERATURE CITED

1. Germain, R. N. 1994. MHC-dependant antigen processing and peptide presentation: providing ligands for T lymphocyte activation. Cell 76:287.

2. Sprent, J. 1989. T lymphocytes and the thymus. Fundamental Immunology 2nd Edition. 69.

3. Hansen T. H., and D.H. Sachs. 1989. The major histocompaibility complex. Fundamental Immunology 2nd Edition. 445.

4. Counce, S., P. Smith, R. Barth, and G.D. Snell. 1956. Strong and weak histocompatibility gene differences in mice and their role in the rejection of homografts of tumor and skin. Ann. Surg. 144:198.

5. Benacerraf, B., and H.O. McDevitt. 1972. Histocompatibility-linked immune response genes. Science 175:273.

6. Schwartz, R. H. 1985. T-lymphocyte recognition of antigen in association with gene products of the major histocompatibility complex. Annu. Rev. Immunol. 3:237.

7. Bjorkman, P. J., M. A. Saper, B. Samraoui, W. S. Bennett, J. L. Strominger, and D. C. Wiley. (1987). Structure of the human class I histocompatibility antigen, HLA-A2. Nature 329:506.

8. Matsumura, M., D. H. Fremont, P. A. Peterson, and I. A. Wilson. 1992. Emerging principles for the recognition of peptide antigens by MHC class I molecules. Science 257:927.

9. Madden, D. R., J. C. Gorga, J. L. Strominger, and D. C. Wiley. 1992. The three-dimensional structure of HLA-B27 at 2.1 A resolution suggests a general mechanism for tight peptide binding to MHC. Cell 70:1035.

10. Falk, K., O. Rotzschke, S. Stevanovich, G. Jung, and H. G. Rammensee. 1991. Allele-specific motifs revealed by sequencing of self peptides eluted from MHC molecules. Nature 351:290.

11. Brown, J. H., T. S. Jardetzky, J. C. Gorga, L. J. Stern, R. G. Urban, J. L. Strominger, and D. C. Wiley. 1993. The three-dimensional structure of the human class II histocompatibility antigen HLA-DR1. Nature 364:33.

12. Rudensky, A., H. P. Preston, S. C. Hong, A. Barlow, and C. J. Janeway. 1991. Sequence analysis of peptides bound to

MHC class II molecules. Nature 353:622.

13. Chicz, R. M., R. G. Urban, J. C. Gorga, W. S. Lane, L. J. Stern, D. A. A. Vignalli, and J. L. Strominger. 1992. Predominant naturally processed peptides bound to HLA-DR1 are derived from MHC-related molecules and are heterogenous in size. Nature 358:764.

14. Hunt, D. F., H. Michel, T. A. Dickinson, J. Shabanowitz, A. L. Cox, K. Sakaguchi, E. Appella, H. M. Grey, and A. Sette. (1992b). Peptides presented to the immune system by the murine class II major histocompatibility complex molecule I-A^d. Science 256:1817.

15. Sette, A., L. Adorini, S. M. Colon, S. Buus, and H. M. Grey. 1989. Capacity of intact proteins to bind to MHC class II molecules. J. Immunol. 143:1265.

16. Weiss, A. 1989. T lymphocyte activation. Fundamental Immunology 2nd Edition. 359.

17. Townsend, A. R., F. M. Gotch, and J. Davey. 1985. Cytotoxic T cells recognize fragments of the influenza nucleoprotein. Cell 42:457.

18. Morrison, L. A., A. E. Lukacher, V. L. Braciale, D. P. Fan, and T. J. Braciale. 1986. Differences in antigen presentation to MHC class I- and class II-restricted influenza virus-specific cytolytic T lymphocyte clones. J. Exp. Med. 163:903.

19. Moore, M. W., F. R. Carbone, and M. J. Bevan. 1988. Introduction of soluble protein into the class I pathway of antigen processing presentation. Cell 54:777.

20. Yewdell, J. W., J. R. Bennink, Y. Hosaka. 1988. Cells process exogenous proteins for recognition by cytotoxic T lymphocytes. Science 239:637.

21. Hunt, D. F., R. A. Henderson, J. Shabanowitz, K. Sakaguchi, H. Michel, N. Sevilir, A. L. Cox, E. Appella, and V. H. Engelhard. 1992a. Characterization of peptides bound to the class I MHC molecule HLA-A2.1 by mass spectrometry. Science 255:1261.

22. Townsend, A., C. Ohlen, J. Bastin, H. G. Ljunggren, L. Foster, and K. Karre. 1989. Association of class I major histocompatibility heavy and light chains induced by viral peptides. Nature 340:443.

23. Monaco, J. J. 1992. Genes in the MHC that may affect antigen processing. Curr. Opin. Immunol. 4:70.

24. Kleijmeer, M. J., A. Kelly, H. J. Geuze, J. W. Slot, A. Townsend, and J. Trowsdale. 1992. Location of MHC-encoded transporters in the endoplasmic reticulum and cis-Golgi. Nature 357:342.

25. Shepard, J. C., T. N. M. Schumacher, P. G. Ashton-

Rickardt, S. Imaeda, H. L. Ploegh, C. A. Janeway Jr, and S. Tonegawa. 1993. TAP1-dependant peptide translocation in vitro is ATP and peptide selective. Cell 74:577.

26. Neefjes, J. J., F. Momburg, and G. J. Hammerling. 1993. Selective and ATP-dependant translocation of peptides by the MHC-encoded transporter. Science 261:769.

27. Goldberg, A. L., and K. L. Rock. 1992. Proteolysis, proteosomes, and antigen presentation. Nature 357:375.

28. Rock, K. L. C. Gramm, L. Rothstein, K. Clark, R. Stein, L. Dick, D. Hwang, and A. L. Goldberg. 1994. Inhibitors of the proteasome block the degradation of most cell proteins and the generation of peptides presented on MHC class I molecules. Cell 78:761.

29. Driscoll, J., M. G. Brown, D. Finley, and J. J. Monaco. 1993. MHC-linked LMP gene products specifically alter peptidase activities of the proteasome. Nature 365:262.

30. Gaczynska, M., K. L. Rock, and A. L. Goldberg. 1993. τ-interferon and expression of MHC genes regulate peptide hydrolysis by proteasomes. Nature 365:264.

31. Fehling, H. J., W. Swat, C. Laplace, R. Kuhn, K. Rajewsky, U. Muller, H. von Boehmer. 1994. MHC class I expression in mice lacking the proteasome subunit LMP-7. Science 265:1234.

32. Momburg, F., V. Ortiz-Navarrete, J. Neefjes, E. Goulmy, Y. van de Wal, H. Spits, S. J. Powis, G. W. Butcher, J. C. Howard, P. Walden, and G. Hammerling. 1992. Proteasome subunits encoded in the major histocompatibility complex are not essential for antigen presentation. Nature 360:174.

33. Arnold, D., J. Driscoll, M. Androlewicz, E. Hughes, P. Cresswell, and T. Spies. 1992. Proteasome subunits encoded in the MHC are not generally required for the processing of peptides bound by MHC class I molecules. Nature 360:171

34. Cresswell, P., R. R. Avva, J. E. Davis, C. A. Lamb, J. M. Riberdy, and P. A. Roche. 1990. Intracellular transport and peptide binding properties of HLA class II glycoproteins. Semin. Immunol. 2:273.

35. Layet, C., and R. N. Germain. 1991. Invariant chain promotes egress of poorly expressed, haplotype-mismatched class II major histocompatibility complex AαAβ dimers from the endoplasmic reticulum/cis Golgi compartment. Proc. Natl. Acad. Sci. USA 88:2346.

36. Anderson, M. S., and J. Miller. 1992. Invariant chain can function as a chaperone protein for class II major histocompatibility molecules. Proc. Natl. Acad. Sci. USA 89:2282.

37. Viville, S., J. Neefjes, V. Lotteau, A. Dierich, M. Lemeur, H. Ploegh, C. Benoist, and D. Mathis. 1993. Mice lacking the MHC class II-associated invariant chain. Cell 72:635.

38. Bikoff, E. K. 1992. Formation of complexes bewteen self-peptides and MHC class II molecules in cells defective for presentation of exogenous protein antigens. J. Immunol. 149:1.

39. Roche, P. A., and P. Cresswell. 1990. Invariant chain association with HLA-DR molecules inhibits immunogenic peptide binding. Nature 345:615.

40. Teyton, L., D. O'Sullivan, P. W. Dickson, V. Lotteau, A. Sette, P. Fink, and P. A. Peterson. 1990. Invariant chain distinguishes between the exogenous and endogenous antigen antigen presentation pathways. Nature 348:39.

41. Long, E. O., T. LaVaute, V. Pinet, and D. Jaraquemada.1994. Invariant chain prevents the HLA-DR-restricted presentation of a cytosolic peptide. J. Immunol. 153:1487.

42. Riberdy, J. M., J. R. Newcomb, M. J. Surman, J. A. Barbosa, and P. Cresswell. 1992. HLA-DR molecules from an antigen-processing mutant cell line are associated with invariant chain peptides. Nature 360:474.

43. Ziegler, H. K., and E. R. Unanue. 1982. Decrease in macrophage antigen catabolism by ammonia and chloroquine is associated with inhibition of antigen presentation to T cells. Proc. Natl. Acad. Sci. USA 78:175.

44. Lotteau, V., L. Teyton, A. Peleraux, T. Nilsson, L. Karlsson, S. L. Schmid, V. Quaranta, and P. A. Peterson. 1990. Intracellular transport of class II MHC molecules directed by invariant chain. Nature 348:600.

45. Seglen, P. O. 1983. Endosomes. Methods Enzymol. 96:737.

46. Helenius, A., I. Mellman, D. Wall, and A. Hubbard. 1983. Trends Biochem. Sci. 8:245.

47. Guagliardi, L. E., B. Koppelman, J. S. Blum, M. S. Marks, P. Cresswell, and F. M. Brodsky. 1990. Co-localization of molecules involved in antigen processing and presentation in an early endocytic compartment. Nature 343:133.

48. McCoy, K. L., J. Miller, M. Jenkins, F. Ronchese, R. N. Germain, and R. H. Schwartz. 1989. Diminshed antigen processing by endosomal acidification mutant antigen-presenting cells. J. Immunol. 143:29.

49. Hopkins, C. R., and L. S. Trowbridge. 1983. Internalization of transferrin and the transferrin receptor in human carcinoma A431 cells. J. Cell Biol. 97:508.

50. McCoy, K. L., M. Noone, J. K. Inman, and R. Stutzman.

1993. Exogenous antigens internalized through transferrin receptors activate CD4$^+$ T cells. J. Immunol 150:1691.

51. Chu, C. T., and S. V. Pizzo. 1993. Receptor-mediated antigen delivery into macrophages: Complexing antigen to α2-macroglobulin enhances presentation to T cells. J. Immunol. 150:1

52. Harding, C. V., D. S. Collins, J. W. Slot, H. J. Geuze, and E. R. Unanue. 1991. Liposome-encapsulated antigens are processed in lysosomes, recycled and presented to T cells. Cell 64:393.

53. Diment, S. 1990. Different roles for thiol and aspartyl proteases in antigen presentation of ovalbumin. J. Immunol. 145:417.

54. Rodriguez, G. M., and S. Diment. 1992. Role of cathepsin D in antigen presentation of ovalbumin. J. Immunol. 149:2894.

55. Bennett, K., T. Levine, J. S. Ellis, R. J. Peanasky, I. M. Samloff, J. Kay, and B. M. Chain. 1992. Antigen processing for presentation by class II major histocompatibility complex requires cleavage by cathepsin E. Eur. J. Immunol. 22:1519.

56. Amigorena, S., J. R. Drake, P. Webster, and I. Mellman. 1994. Transient accumulation of new class II MHC molecules in a novel endocytic compartment in B lymphocytes. Nature 369:113.

57. Tulp, A., D. Verwoerd, B. Dobberstein, H. L. Ploegh, and J. Pieters. 1994. Isolation and characterization of the intracellular MHC class II compartment. Nature 369:120.

58. West, M. A., J. M. Lucocq, and C. Watts. 1994. Antigen processing and class II MHC peptide-loading compartments in human B-lymphoblastoid cells. Nature 369:147.

59. Qiu, Y., X. Xu, A. Wandinger-Ness, D. P. Dalke, and S. K. Pierce. 1994. J. Cell Biol. 125:595.

60. Ljunggren, H. G., N. J. Stam, C. Õhlén, J. J. Neefjes, P. Hõglund, M. T. Heemels, J. Bastin, T. N. M. Schumacher, A. Townsend, K. Kärre, and H. L. Ploegh. 1990. Empty MHC class I molecules come out in the cold. Nature 346:476.

61. Spies, T. and R. Demars. 1991. Restored expression of major histocompatibility class I molecules by gene transfer of a putative peptide transporter. Nature 351:323.

62. Mellins, E., L. Smith, B. Arp, T. Cotner, E. Celis, and D. Pious. 1990. Defective processing and presentation of exogenous antigens in mutants with normal HLA class II genes. Nature 343:71.

63. Mellins, E., S. Kempin, L. Smith, T. Monji, and D. Pious. 1991. A gene required for class II-restricted antigen presentation maps to the major histocompatibility complex. J.Exp. Med. 174:1607.

64. Morris, P., J. Shaman, M. Attaya, M. Amaya, S. Goodman, C. Bergman, J. J. Monaco, and E. Mellins. 1994. An essential role for HLA-DM in antigen presentation by class II major histocompatibility molecules. Nature 368:551.

65. Fling, S. P., B. Arp, and D. Pious. 1994. HLA-DMA and DMB genes are both required for MHC class II/peptide complex formation in antigen-presenting cells. Nature 368:554.

66. Jensen, P. E. 1991. Reduction of disulfide bonds during antigen processing: evidence for a thiol-dependant insulin determinant. J. Exp. Med. 174:1121.

67. Collins, D. S., E. R. Unanue, and C. V. Harding. 1991. Reduction of disulfide bonds within lysosomes is a key step in antigen processing. J. Immunol. 147:4054.

68. Maillère, B., J. Cotton, G. Mourier, M. Léonetti, S. Leroy, and A. J. Ménez. 1993. Role of thiols in the presentation of a snake toxin to murine T cells. J.Immunol. 150:270.

69. Lloyd, J. B. 1986. Disulfide bond reduction in lysosomes: the role of cysteine. Biochem. J. 237:271.

70. Shimonkevitz, R., S. Colon, J. W. Kappler, P. Marrack, and H. N. Grey. 1984. Antigen recognition by H-2-restricted T cells. II. A tryptic ovalbumin peptide that substitutes for processed antigen. J.Immunol. 133:2067.

71. Guillet, J. G., M. Z. Lai, T. J. Briner, J. A. Smith, and M. L. Gefter. 1986. Interaction of peptide antigens and class II major histocompatibility complex antigens. Nature 324:260.

72. Jensen, P. E. 1993. Acidification and disulfide reduction can be sufficient to allow intact proteins to bind class II MHC. J. Immunol. 150:3347.

73. Glimcher, L. G., T. Hamano, R. Asofsky, E. Heber-Katz, S. Hedrick, R. H. Schwartz, and W. E. Paul. 1982. I region-restricted antigen presentation by B cell-B lymphoma hybridomas. Nature 298:283.

74. Kappler, J., J. White, D. Wegmann, E. Mustain, and P. L. Marrack. 1982. Antigen presentation by Ia^{+} B cell hybridomas to H-2-restricted T cell hybridomas. Proc. Natl. Acad. Sci. USA 79:3604.

75. Baker, P. E., S. Gillis, and K. A. Smith. 1979. Monoclonal cytolytic T cell lines. J. Exp. Med. 149:273.

76. Kappler, J. W., B. Skidmore, J. White, and P. Marrack. 1981. Antigen inducible H-2-restricted interleukin-2-

producing T cell hybridomas. Lack of independent antigen and H-2 recognition. J. Exp. Med. 153:1198.

77. Lerner, E. A., L. A. Matis, C. A. Janeway Jr., P. P. Jones. R. H. Schwartz, and D. B. Murphy. 1980. Monoclonal antibody against an Ir gene product? J. Exp. Med. 152:1085.

78. Ozato, K., T. H. Hansen, and D. H. Sachs. 1980. Monoclonal antibodies to mouse MHC antigens. II. Antibodies to the H-2L^d ntigen, and the products of a third polymorphic locus of the mouse major histocompatibility complex. J. Immunol. 125:2473.

79. Lanier, L. L., G. A. Gutman, D. E. Lewis, S. T. Griswold, and N. L. Warner. 1982. Monoclonal antibodies against rat Ig kappa chains. Hybridoma 1:125.

80. Koch, N., S. Koch, and G. J. Hämmerling. 1982. Ia invariant chain detected on lymphocyte surfaces by monoclonal antibody. Nature 299:644.

81. Diment, S., M. S. Leech, and P. D. Stahl. 1988. Cathepsin D is membrane-associated in macrophage endosomes. J. Biol. Chem. 263:6901.

82. Lee, C. L., and M. Z. Atassi. 1973. Conformation and immunochemistry of methylated and carboxymethylated derivatives of lysozyme. Biochemistry. 12:2690.

83. Chestnut, R.W., R. O. Endres. and H. M. Grey. 1980. Antigen recognition by T cells and B cells: Recognition of cross-eactivity between native and denatured forms of globular ntigens. Clin. Immunol. Immunopathol. 15:397.

84. Feener E. P., W. C. Shen, and H. J.-P. Ryser. 1990. Cleavage of disulfide bonds in endocytosed macromolecules. J. Biol. Chem. 265:18780.

85. Gaitonde, M. K. 1967. A spectrophotometric method from the direct measurement of cysteine in the presence of other naturally occurring amino acids. Biochem. J. 104:627.

86. Tietze, F. 1969. Enzymic method for quantitative determination of nanogram amounts of total and oxidized glutathione: applications for mammalian blood and other tissues. Anal. Biochem. 27:502.

87. Pisoni, R. L., T. L. Acker, K. M. Lisowski, R. M. Lemons, and J. G. Thoene. 1990. A cysteine-specific lysosomal transport system provides a major route for the delivery of thiol to human fibroblast lysosomes: possible role in supporting lysosomal proteolysis. Journal Cell Biol. 110:327.

88. Lechler, R. I., F. Ronchese, N. S. Braunstein, and R. N. Germain. 1986. I-A-restricted T cell antigen recognition: analysis of the roles of A_α and A_β using DNA-mediated gene transfer. J. Exp. Med. 163:678.

89. Yim, C. Y., J. B. Hibbs jr, J. R. McGregor, R. E. Galinsky, and W. E. Samlowski. 1994. Use of N-acetyl cysteine to increase intracellular glutathione during the induction of antitumor responses by IL-2. J. Immunol. 152:5796.

90. Yamashita, K., Y. Tachibana, and A. Kobata. 1978. The structures of the galactose-containing sugar chains of ovalbumin. J. Biol. Chem. 253:3862.

91. Tai, Tadashi., K. Yamashita, M. Ogata-Arakawa, N. Koide, T. Muramatsu, S. Iwashita, Y. Inoue, and A. Kobata. 1975. Structural studies of two ovalbumin glycopeptides in relation to the Endo-β-N-acetylglucosaminidase specificity. J. Biol. Chem. 21:8569.

92. Romagnoli, P., C. Layet, J. Yewdell, O. Bakke, and R. N. Germain. 1993. Relationship between invariant chain expression and major histocompatibility complex class II transport into early and late endocytic compartments. J. Exp. Med. 177:583.

93. Cresswell, P. 1985. Intracellular class II HLA antigens are accessible to transferrin neuraminidase conjugates internalized by receptor-mediated endocytosis. Proc. Natl. Acad. Sci. USA 82:8188.

94. Mego, J. L. 1984. Role of thiols, pH and cathepsin D in the lysosomal catabolism of serum albumin. Biochem. J. 218:775.

95. Hampl, J., G. Gradehandt, h. Kalbacher, and E. Rüde. 1992. In vitro processing of insulin for recognition by murine T cells results in the generation of A chains with free CysSH. J. Immunol. 148:2664.

96. Shimonkevitz, R., J. Kappler, P. Marrack, and H. Grey. 1983. Antigen recognition by H-2-restricted T cells. I. Cell-free antigen processing. J. Exp. Med. 158:303.

97. Vidard, I., K. L. Rock, and B. Benacerraf. 1992. Diversity in MHC class II ovalbumin T cell epitopes generated by distinct proteases. J. Immunol. 149:498.

98. Streicher, H. Z., I. J. Berkower, M. Busch, F. R. N. Gurd, and J. Berzofsky. 1984. Antigen conformation determines processing requirements for T cell activation. Proc. Natl. Acad. Sci. USA 81:6831.

99. Régnier-Vigouroux, A. R., Ayeb, M. L. Defendini, C. Granier, and M. Pierres. 1988. Processing by accessory cells for presentation to murine T cells of apamin, a disulfide bonded 18 amino acid peptide. J. Immunol. 140:1069.

100. Allen, P. M., and E. R. Unanue. 1984. Different requirements for antigen processing by macrophages for lysozyme-specific T cell hybridomas. J. Immunol. 132:1077.

VITA

[redacted]